frontiers | Frontiers in Sustainable Food Systems

TYPE Original Research
PUBLISHED 01 November 2024
DOI 10.3389/fsufs.2024.1500278

OPEN ACCESS

EDITED BY
Guihun Jiang,
Jilin Medical University, China

REVIEWED BY
Tran Van Cuong,
Tay Nguyen University, Vietnam
Xiaowen Hu,
Wenzhou Medical University, China

*CORRESPONDENCE
Zhengyu Hu
✉ huzhengyu1994@163.com
Gao Li
✉ gli@ybu.edu.cn

†These authors share first authorship

RECEIVED 23 September 2024
ACCEPTED 24 October 2024
PUBLISHED 01 November 2024

CITATION
Xu W, Zhou W, Sun J, Chen W, Wu X, Guan T, Zhao Y, Yang P, Hu Z and Li G (2024) Isolation, structural characterization, and hypoglycemic activity of polysaccharides from the stems of *Panax ginseng* C. A. Meyer.
Front. Sustain. Food Syst. 8:1500278.
doi: 10.3389/fsufs.2024.1500278

Isolation, structural characterization, and hypoglycemic activity of polysaccharides from the stems of *Panax ginseng* C. A. Meyer

Weiwei Xu†, Wei Zhou†, Jinfeng Sun, Weiwei Chen, Xuanye Wu, Tong Guan, Yilin Zhao, Pengcheng Yang, Zhengyu Hu* and Gao Li*

Key Laboratory of Natural Medicines of the Changbai Mountain, Ministry of Education, College of Pharmacy, Yanbian University, Yanji, China

The purpose of this study was to obtain polysaccharides from *Panax ginseng* C. A. Meyer stems (PGSPs), agro-byproducts with development potential, and fully explore the potential value in *P. ginseng* stems. Two novel polysaccharides firstly from *P. ginseng* stems (PGSP-1 and PGSP-2) were obtained by water extraction and alcohol precipitation method and column chromatography, and then characterized by FT-IR, HPGPC, HPLC, SEM, TGA, GC–MS and NMR. The results demonstrated that PGSP-1 (Mw = 723.83 kDa) and PGSP-2 (Mw = 620.48 kDa) were characterized →4)-β-D-Gal*p*-(1→, →6)-α-D-Glc*p*-(1→ and →2)-α-L-Rha*p*-(1→ as the skeleton, →4,6)-β-D-Gal*p*-(1→ and →2,6)-α-D-Man*p*-(1→ as the cross junction, α-L-Araf-(1→ as the terminal unit, and PGSP-1 still contained →4)-β-D-Gal*p*, while PGSP-2 contained →4)-β-D-Xyl*p*-(1→, →3)-β-D-Glc*p*A-(1→, →4)-β-D-Gal*p*A-(1→) and α-D-Glc*p*-(1→, with different microstructures and thermal stability. And the results of hypoglycemic activity revealed that both PGSP-1 and PGSP-2 showed excellent inhibitory activity against α-glucosidase and α-amylase, in which PGSP-2 had the better performance. The inhibition kinetics result showed that PGSPs on α-glucosidase and α-amylase were non-competitive type and mixed type inhibition. This study provided a theoretical basis for making full use of and exploiting the economic value of agro-byproducts such as *P. ginseng* stems and offered a theoretical reference for the effective utilization of PGSP as a functional component to prevent and reduce T2DM.

KEYWORDS

agro-byproducts, *Panax ginseng* C. A. Meyer stems, polysaccharides, preparation, hypoglycemic

1 Introduction

Polysaccharides, which are carbohydrates composed of more than ten monosaccharides linked by glycosidic bonds, widely exist in plants, animals and microorganisms (Lv et al., 2021), in which plant polysaccharides have received a great deal of attention due to their pharmacological activities. Recently, Zhou et al. (2023), Wang J. W. et al. (2024), and Jiang et al. (2024) found that polysaccharides could regulate the intestinal microbiota and then exerted hypoglycemic effects against diabetes mellitus (Chen J. C. et al., 2023), as well as Pi et al. (2024), Zhang J. et al. (2024), Faidi et al. (2025), and Ghosh and Abdullah (2024) demonstrated that polysaccharides possesed anti-virus, which proved that polysaccharides were of great

research value. In addition, studies had shown that agro-byproducts well-known also contained different contents of polysaccharides (Sila et al., 2014; Lv, 2020). However, it is a pity that most agro-byproducts, which deserved the attention of researchers on account of its advantages of low-cost and easy-collect, are often discarded as a result of not as the main medicinal parts. Therefore, it is of great significance to try to focus on exploiting potential value of agro-byproducts from the perspective of polysaccharides and develop them into potential functional foods with protective effects.

Panax ginseng C. A. Meyer stems are the dried stems from *P. ginseng*, a plant belonging to *Araliaceae* family, which are the agro-byproducts during harvesting process of *P. ginseng*, and mainly distributed in China, Russia, South Korea, North Korea and Japan (Guo et al., 2021). *P. ginseng* stems rich in a variety of active ingredients including ginsenosides, polysaccharides, volatile oils, flavonoids, triterpenes and amino acids, and possess various pharmacological effects such as anti-oxidation, hypoglycemic and immune regulation. Nevertheless, the dried roots, rhizomes and dried leaves from *P. ginseng* are widely harvested as a result of the medicinal parts of *P. ginseng*, while the stems of *P. ginseng*, another part in *P. ginseng*, are discarded frequently in the process of harvesting, failing to explore the potential value of *P. ginseng* stems, resulting in waste of resources and environmental pollution. Therefore, if the potential value of *P. ginseng* stems can be fully exploited, it will bring economic benefits to the society as well as reduce the problem of environmental pollution caused by the waste of resources. And it is very pleasing and gratifying that polysaccharides, as one of the main active components in *P. ginseng* stems, have been proved that they possess excellent pharmacological activity (Zhang X. H. et al., 2024), which provides strong evidence support for the development of *P. ginseng* stems polysaccharides. However, the research on *P. ginseng* stems polysaccharides still remained in the study of crude polysaccharides lacking of futher isolation, purification and detailed structural characterization (Zhang Y. et al., 2024). Hence, it is very meaningful to carry out more profound isolation, purification and detailed structural characterization of *P. ginseng* stems polysaccharides and explore the medicinal value and potential activity.

Type 2 diabetes mellitus (T2DM) is a chronic metabolic disease, mainly caused by elevated blood glucose, which can lead to many serious complications, including hyperlipidemia, atherosclerosis, cardiovascular disease and renal failure (Zhao et al., 2021). The α-glycosidase and α-amylase are the key enzymes in the process of carbohydrate digestion. When the body ingests carbohydrates, α-glycosidase and α-amylase hydrolyze them into disaccharides or monosaccharides, which are absorbed by the small intestine and eventually enter the blood causing elevated blood glucose (Bai, 2023). Studies have shown that inhibition of α-glycosidase and α-amylase involved in carbohydrate hydrolysis is an effective therapeutic method on T2DM (Fu et al., 2020). At present, the acarbose and other commercial drugs are widely used to reduce blood glucose levels, but long-term use may lead to a variety of side effects (Zhang F. et al., 2023). Natural polysaccharides have attracted increasing attention due to their unique physical and chemical properties, non-toxicity and remarkable physiological activity (Liu et al., 2015). More and more studies have evidenced that natural polysaccharides with different structures can effectively inhibit the activity of α-glycosidase and α-amylase to achieve the effect of lowering blood glucose (Chen et al., 2024; Tang et al., 2023; Tian et al., 2023), while the hypoglycemic activity of polysaccharides from *P. ginseng* stems has not been reported yet.

Therefore, in this study, two novel polysaccharides firstly from *P. ginseng* stems (PGSP-1 and PGSP-2) were obtained by water extraction and alcohol precipitation method and column chromatography, and then characterized by FT-IR, HPGPC, HPLC, SEM, TGA, GC–MS, and NMR, and futher studied the inhibitory activity and kinetics of PGSPs on α-glycosidase and α-amylase. This study aims to provide a theoretical reference for effective utilization of PGSPs from *P. ginseng* stems as healthy products with hypoglycemic activity against T2DM, and also to attract more and more attention to the potential economic value on the agro-byproducts such as *P. ginseng* stems.

2 Materials and methods

2.1 Materials and reagents

The dried stems of *Panax ginseng* C.A. Meyer were collected from Yanbian Ginseng Research Institute (Yanji, China), and authenticated by GL. The voucher specimen (voucher number: YB-PGS-20211201) has been deposited at Yanbian University. Mannose (Man), ribose (Rib), rhamnose (Rha), glucosamine (GlcN), glucose (Glc), xylose (Xyl), arabinose (Ara), glucuronic acid (GlcA), galacturonic acid (GalA), galactose (Gal) and fucose (Fuc) were bought from Shanghai Aladdin Bio-Chem Technology Co., LTD. (Beijing, China). Dextran with different molecular weights (National drug reference material) was purchased from China Foods Limited and Drug Control Institute. The α-glucosidase, α-amylase, *p*-nitrophenyl-α-D-glucopyranoside and acarbose were purchased from Shanghai yuanye Bio-Technology Co., Ltd. (Shanghai, China).

2.2 Isolation and purification of polysaccharides

The approach of water-extraction and alcohol-precipitation was performed to obtain polysaccharides from *Panax ginseng* C. A. Mey. (PGSP) as described previously (Yuan et al., 2024). In brief, the dried *P. ginseng* stems were cut into small segments of 1–2 cm after removing impurities and mixed with distilled water at a liquid–solid ratio of 27:1 (mL/g), as well as condensation reflux extraction at 85°C for 2.9 h. The obtained aqueous extract was filtered and the filtrate was concentrated to one-fifth of the original volume. Subsequently, a certain amount of ethanol was added to make the final concentration of ethanol in the solution up to 85%, during which sufficient stirring was carried out in order to ensure that the polysaccharides could be effectively leached from the solution. It was then kept at 4°C for 12 h, and centrifuged at 3000 rpm for 10 min to collect precipitate which was dried and ground to obtain crude PGSP. The purification procedure was conducted utilizaing Sevag method (Hu et al., 2022) to eliminate protein and gained deproteinated PGSP.

Futher, the deproteinated PGSP was isolated and purified via DEAE-52 cellulose column (Li et al., 2021) and Sephadex G-200 gel filtration column (Ma et al., 2014), respectively. The power (1 g) of PGSP was dissolved in appropriate distilled water and loaded onto a DEAE-52 cellulose column (26 mm × 300 mm), eluting with distilled

water and a gradient of 0.1, 0.2, 0.3, 0.4, and 0.5 mol/L NaCl solution at a flow rate of 1 mL/min. All eluents (5 mL/tube, 25 tubes/gradient) were monitored by the phenol-sulfuric acid method (Yu et al., 2022) at 490 nm. Based on the elution curve, the eluents with the identical absorption peak were collected, concentrated and dialyzed in dialysis bags (cut-off 3,500 Da) with distilled water for 48 h. The dialyzed PGSP was purified using the identical method on a Sephadex G-200 gel filtration column (26 mm × 300 mm) with distilled water at a flow rate of 0.4 mL/min. The eluents (5 mL/tube, 20 tubes/fraction) with the same absorption peaks were pooled, concentrated and lyophilized so as to obtain the purified homogeneous polysaccharide for further characterization.

2.3 Structure characterization

2.3.1 Chemical analysis

The total sugar content of PGSP was determined by phenol-sulfuric acid method with glucose as the standard; The Bradford method was used to measure the protein content of PGSP, and bovine serum albumin as the standard (Bradford, 1976). The uronic acid content of PGSP was analyzed utilizing m-hydroxybiphenyl colorimetric method with galacturonic acid as the standard (Blumenkrantz and Asboe-Hansen, 1973).

2.3.2 UV and FT-IR spectra analysis

PGSP (1 mg/mL) was dissolved in distilled water. The UV absorption of PGSP was measured via a UV (Wu J. Y. et al., 2024) spectrophotometer (UV2600, Techcomp, China) in the wavelength range of 200–800 nm. The power (2 mg) of PGSP was milled with KBr fully and compressed into a transparent sheet. The characteristic absorption peaks of the functional groups were recorded by FT-IR (Zhang J. et al., 2024) spectroscopy (Nicolet iS20, Thermo Scientific, USA) at a range of 4,000–400 cm^{-1}.

2.3.3 Determination of the molecular weight and distributive coefficient

The molecular weight and distributive coefficient (Cai et al., 2023) of PGSP was determined by high-performance gel permeation chromatography (HPGPC) (BOCL104, SHIMADZU, Japan) equipped with a refractive index detector-20A (RID-20A) using a column (Shodex SUGAR KS-804, 8.0 mm × 300 mm, Shimadzu, Janpan) which maintained at 40°C and eluted with ultrapure water at a flow rate of 1 mL/min. Briefly, the standard curve was plotted using dextran with different molecular masses (9.75, 36.8, 64.65, 135.35, and 300.6 kDa) as standards, and the linear regression equation ($logMw = -0.58\,T + 8.86$) was obtained. A certain amount of PGSP was dissolved in ultrapure water to obtain polysaccharide solution (1 mg/mL) and filtered by a filter of 0.45 μm pore size for the subsequent analysis. The sample injection was 20 μL. Based on the retention time of PGSP, the molecular weight and distributive coefficient were calculated by LabSolutions software using linear regression equation.

2.3.4 Monosaccharide composition analysis

The monosaccharide composition of PGSP was analyzed via high-performance liquid chromatography (HPLC) (Primaide, HITACHI, Japan) equipped with an UV detector (1,410 UV Detector) and a column (Supersil ODS2 5 μm, 4.6 mm × 150 mm) maintained at 35°C using the pre-column derivatization method (Shao et al., 2023) with minor modifications as reported previously. Briefly, the powder (10 mg) of PGSP sample was hydrolyzed with trifluoroacetic acid (TFA) (2 mL, 2 mol/L) at 120°C for 6 h. Cooling to room temperature, the hydrolyzed sample was mixed with methanol, concentrated and dried in order to remove TFA completely. Subsequently, the sample was redissolved in distilled water (400 μL), and 200 μL was taken out to be derivatized with NaOH solution (200 μL, 0.3 mol/L) and 1-phenyl-3-methyl-5-pyrazolone (PMP) (200 μL, 0.5 mol/L) at 70°C for 1 h. After cooling, HCl solution (200 μL, 0.3 mol/L) was added to terminate the reaction. It was then extracted by chloroform three times, and the aqueous layer was collected and filtered by a filter of 0.45 μm pore size. The filtered sample was analyzed via HPLC and eluted by a mixture of 83% phosphate buffer solution (pH 6.8, phosphate buffer solution: acetonitrile = 83: 17) at a flow rate of 1.0 mL/min. The detector wavelength was set to 245 nm.

2.3.5 Scanning electron microscopy analysis (SEM)

Scanning electron microscope (Gemini SEM 360, ZEISS, Germany) was used to observe the surface morphology and microstructure of PGSP. A certain amount of PGSP sample was adhered to the specimen stage, on which a thin layer of gold coating was spread. Then SEM analysis (Ghamgui et al., 2024) was carried out at the magnification of 1,000 ×, 5,000 × and 15,000 ×.

2.3.6 Thermogravimetric analysis (TGA)

The variable relationship between mass and temperature of PGSP was evaluated by TGA (Qiu et al., 2024) machine (TG 209 F1 Libra, NETZSCH, Germany). An amount of PGSP was put on pallet, and heated from 30°C to 800°C at the heating rate of 20°C/min under 20 mL/min nitrogen flow, and then analyzed by means of TGA.

2.3.7 Methylation analysis

The methylation analysis was carried out to determine glycosidic bond linkage pattern of the purified PGSP as described previously with slight modifications (Sims et al., 2018). In detail, the NaOH (240 mg) solid was added to DMSO (12 mL) solution and milled thoroughly to obtain NaOH-DMSO suspension, then the powder (40 mg) of PGSP was added into it and dissolved by ultrasounding in a nitrogen atmosphere. It was then kept in ice bath, added methyl iodide (3 mL) and ultrasounded for 40 min, which was repeated three times so as to methylate fully. The methylation reaction was terminated by the addition of distilled water (2 mL) to the residue and then dialyzed in dialysis bags (cut-off 3,500 Da) with distilled water for 48 h. The residue was extracted by chloroform and water in order each three times, as well as all chloroform layers were dried with anhydrous sodium sulfate for 24 h. After concentration to dryness, the premethylation product was hydrolyzed with TFA (6 mL, 2 mol/L) at 110°C for 3 h and concentrated to dryness with anhydrous methanol. Then, the hydrolysate was reduced with $NaBH_4$ (6 mL, 2 mol/L) at room temperature for 3 h, during which oscillated it several times and then kept overnight. At the end of the reaction, it was dropwise added with glacial acetic acid and adjusted pH to 5.5–7.0. After concentration to dryness, the reduction product was acetylated via mixed solution of pyridine and acetic anhydride (4 mL, 1: 1), sealed and reacted at 100°C for 2 h. The residue was concentrated to dryness, redissolved in distilled water and extracted by chloroform as well as aqueous layer

was concentrated to dryness so as to obtain partially methylated alditol acetates (PMAAs).

Subsequently, the PMAAs was redissolved in chloroform and analyzed by gas chromatography–mass spectroscopy (GC–MS) equipped with a DM-5MS column (30 m × 0.32 mm × 0.25 μm). The temperature program was set as: (1) 140°C as initial temperature for 2 min; (2) increasing to 200°C at 2°C/min and maintaining 2 min; (3) increasing to 280°C at 10°C/min and maintaining 5 min. Helium was used as carrier gas at a rate of 1 mL/min.

2.3.8 NMR analysis

^{1}H NMR, ^{13}C NMR and HSQC spectra of PGSP were acquired by 500 MHz nuclear magnetic resonance (NMR) spectrometer (Li et al., 2023) so as to characterize polysaccharide structures fully as described method previously. The dried purified powdr (30 mg) of PGSP was dissolved into D_2O (600 μL) and then determined by means of NMR.

2.4 Determination of hypoglycemic activities *in vitro*

2.4.1 α-glucosidase inhibitory activity assay

The inhibitory activity assay of PGSP on α-glucosidase was performed using the method with minor modifications (Guo et al., 2023) as described previously. Briefly, the PGSP solution of different concentrations (0.2–1.0 mg/mL), α-glucosidase solution (1 U/mL) and *p*-nitrophenyl-α-D-glucopyranoside (pNPG) (5.0 mmol/L) were prepared by phosphate buffer solution (0.2 mol/L, pH 6.8). The phosphate buffer solution (100 μL) was put into a 96-well plate, then the PGSP solution (20 μL) was mixed with α-glucosidase solution (20 μL) and incubated at 37°C for 15 min. The reaction was activated by the addition of pNPG (20 μL) as well as the mixed system was incubated at 37°C for 15 min. To terminate the reaction, sodium carbonate solution (80 μL, 0.2 mol/L) was added and the absorption was monitored at 405 nm. Acarbose (0.2–1.0 mg/mL) was used as a positive control. The inhibition rate of α-glucosidase was calculated by the following Equation 1:

$$\alpha-\text{glucosidase inhibition rate}(\%) = \left[1-(A_1-A_2)/A_3-A_0\right]\times 100 \quad (1)$$

where A_1 was the absorbance of the mixed solution (including sample, enzyme, pNPG, and buffer solution), A_2 was the absorbance of the mixed solution without pNPG, A_3 was the absorbance of the mixed solution without sample and A_0 was the absorbance of the mixed solution without sample and pNPG.

2.4.2 α-amylase inhibitory activity assay

The inhibitory activity assay of PGSP against α-amylase was conducted through the earlier method with slight modifications (Chen et al., 2024). Similarly, the PGSP solution of different concentrations (0.2–1.0 mg/mL) and α-amylase solution (1 U/mL) were prepared with phosphate buffer solution (0.2 mol/L, pH 6.8). The PGSP solution (1 mL) was mixed with α-amylase solution (100 μL) and incubated at 37°C for 20 min. The reaction was initiated by the additoin of starch solution (100 μL, 1%, w/v) and incubated at 37°C for 15 min. The mixed system was added with DNS solution (375 mL) and it was then kept in boiling water bath for 10 min. Cooling to room temperature, the supernatant was obtained after centrifugation and diluted with phosphate buffer solution (3 mL), and then the absorption was determined at 540 nm. Acarbose (0.2–1.0 mg/mL) as a positive control. The inhibition rate of α-amylase was calculated by the following Equation 2:

$$\alpha-\text{amylase inhibition rate}(\%) = \left[1-(A_1-A_2)/A_3-A_0\right]\times 100 \quad (2)$$

where A_1 was the absorbance of the mixed solution (including sample, enzyme, starch and DNS), A_2 was the absorbance of the mixed solution without starch, A_3 was the absorbance of the mixed solution without sample and A_0 was the absorbance of the mixed solution without sample and starch.

2.4.3 Inhibition kinetic analysis

The inhibitory kinetics of PGSP on α-glucosidase and α-amylase was carried out by means of Michaelis–Menten equation and Lineweaver-Burk plots (Niu et al., 2023) as described previously. The experiment operations were carried out utilizing identical method of the above-mentioned inhibitory activity assay with the PGSP solution (0.2, 0.4 and 0.8 mg/mL), α-glucosidase solution (1 U/mL) and pNPG solution (different concentrations) for α-glucosidase, as well as the PGSP solution (0.2, 0.4 and 0.8 mg/mL), α-amylase solution (1 U/mL) and starch solution (different concentrations) for α-amylase, respectively. Double-reciprocal curves of Lineweaver-Burk were plotted for determining the inhibitory kinetics of PGSP against α-glucosidase and α-amylase, and the Equation 3 was expressed as:

$$\frac{1}{v} = \frac{K_m}{V_{\max}}\cdot\frac{1}{[S]} + \frac{1}{V_{\max}} \quad (3)$$

where v and [S] stood for enzyme reaction rate and concentrations of substrates, respectively, Vmax and Km represented by the maximum reaction rate and Michaelis–Menten constant, respectively, as well as 1/v could denoted by the linear Cornish-Bowden-Eisenthal plot (Equation 4),

$$\frac{1}{v} = \frac{K_m}{Vmax}\cdot\left(1+\frac{[I]}{K_i}\right)\cdot\frac{1}{[S]} + \frac{1}{V_{\max}}\cdot\left(1+\frac{[I]}{K_{ii}}\right) \quad (4)$$

where [I] and [S] represented by the concentrations of inhibitor and substrate, respectively, K_i denoted the dissociation constant of enzyme-inhibitor (EI) complexes into inhibitor (I) and enzyme (E), and K_{ii} denoted the inhibition constant of enzyme-substrate-inhibitor (ESI) complexes into enzyme-substrate (ES) complexes.

2.5 Statistical analysis

All data were presented as mean ± standard deviation (SD), with measurements made in triplicate. One-way or two-way ANOVA was performed using SPSS (version 27.0, SPSS Inc., Chicago, USA), and

Michaelis–Menten equation and Lineweaver-Burk was carried out by Origin 2021, and $p < 0.5$ were considered statistically significant.

3 Results and discussion

3.1 Isolation and purification of polysaccharides

The deproteinized PGSP was isolated via DEAE-52 cellulose column eluting with distilled water and a gradient of 0.1, 0.2, 0.3, 0.4, and 0.5 mol/L NaCl solution. As shown in Figure 1A, there were two elution peaks eluted by distilled water and 0.1 mol/L NaCl solution, respectively. Then, the elutions with identical absorption were pooled, concentrated, dialyzed and dried obtaining two polysaccharide fractions which were designated as PGSP-1 (eluted by distilled water) and PGSP-2 (eluted by 0.1 mol/L NaCl solution). According to the isolation principle of DEAE-52, it could be seen that PGSP-1 was a neutral polysaccharide which was uncharged and not easily adsorbable by DEAE-52, thus it was first eluted down by distilled water. PGSP-2 was an acidic polysaccharide negatively charged, which had a strong affinity with DEAE-52, and it was eluted by 0.1 mol/L NaCl solution on account of low uronic acid content. Futher, PGSP-1 and PGSP-2 were purified by Sephadex G-200 gel filtration column eluting with distilled water. As shown in Figure 1B, there was only one elution peak in the elution curve indicating that PGSP-1 and PGSP-2 both were homogeneous polysaccharides. Subsequently, elutions with the same elution peak were pooled, concentrated, dialyzed and dried to acquire dried homogeneous PGSP-1 (245 mg) and PGSP-2 (134 mg) for the next structural characterization.

3.2 Structure characterization

3.2.1 Chemical analysis

The total sugar contents of PGSP-1 and PGSP-2 were calculated to be 93.46 ± 1.02% and 90.81 ± 0.79%, respectively. Compared to previous studies, Wang (2021), Zhao et al. (2009) and Chen and Huang (2019) obtained polysaccharides from *P. ginseng* stems and leaves and *P. ginseng* stems using the identical method, while total sugar contents were far less than PGSP-1 and PGSP-2, demonstrating that the two had rather high purity. The uronic acid content of PGSP-2 was 7.49 ± 0.65%, whereas no uronic acid was detected in PGSP-1, indicating that PGSP-1 was neutral polysaccharide and PGSP-2 was acidic polysaccharide. And the results of uronic acid content analysis further verified the reason for the order of isolation of PGSP-1 and PGSP-2 by DEAE-52. Additionally, no protein was examined both in PGSP-1 and PGSP-2, evidencing that the protein in PGSP had been removed by Sevag method.

3.2.2 UV and FT-IR analysis

The UV spectrum of PGSP-1 and PGSP-2 was shown in Figure 2A, and there were no absorbance peaks at 260 and 280 nm, futher indicating that no proteins and nucleic acids existed in PGSP-1 and PGSP-2. As demonstrated in Figure 2B, it revealed polysaccharide typical absorption peaks of PGSP-1 and PGSP-2 FT-IR spectra ranging from 4,000 to 400 cm^{-1}, and there had a hign degree of similarity between their FT-IR spectra. The strong and broad absorption peak at 3412 cm^{-1} was attributed to O-H stretching vibration (Arab et al., 2021; Han et al., 2024) and the absorption peak at 2937 cm^{-1} was corresponded to C-H stretching vibration (Li et al., 2020), which belonged to polysaccharide characteristic functional groups. The absorption peak at 1607 cm^{-1} was on count of C-O stretching vibration (Shi et al., 2022). Meanwhile, the absorption peak at 1417 cm^{-1} was assigned to C-H asymmetric bending vibration (Alboofetileh et al., 2019), as well as a weak absorption peak around 1,249 cm^{-1} was ascribed to O-H vibration (Wu et al., 2018). The tiny absorption peaks observed at the range of 1,200 to 1,000 cm^{-1} were dued to the overlap of ring vibration, C-O-C glycosidic bond vibration and C-O-H side group stretching vibration, indicating the existence of pyranose (Hong et al., 2021). The absorption peaks near 917 and 831 cm^{-1} implied that both α-configuration and β-configuration of sugar units existed in PGSP-1 and PGSP-2 (Shao et al., 2023). In addition, it was noteworthy that there was a absorption peak near 1730 cm^{-1} owning to C=O stretching vibration (Zhang L. et al., 2023), illustrating that uronic acid existed in PGSP-2 which was consistent with the above-mentioned results of determination of uronic acid content and monosaccharide composition analysis.

3.2.3 Molecular weight and distributive coefficient analysis

The HPGPC chromatogram of PGSP-1 and PGSP-2 was exhibited in Figure 3, which both showed a single symmetrical peak. On account

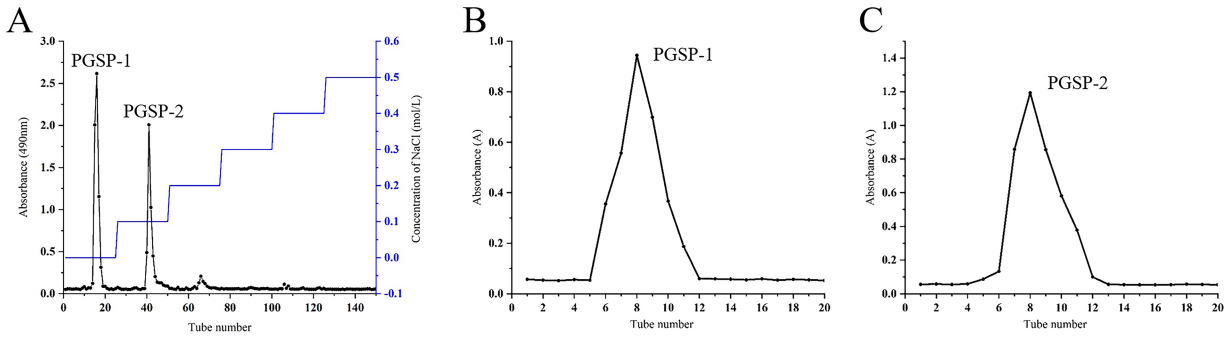

FIGURE 1
Elution curve of PGSP-1 and PGSP-2 on DEAE-52 cellulose column (A), elution curves of PGSP-1 (B) and PGSP-2 (C) on Sephadex G-200 gel filtration column.

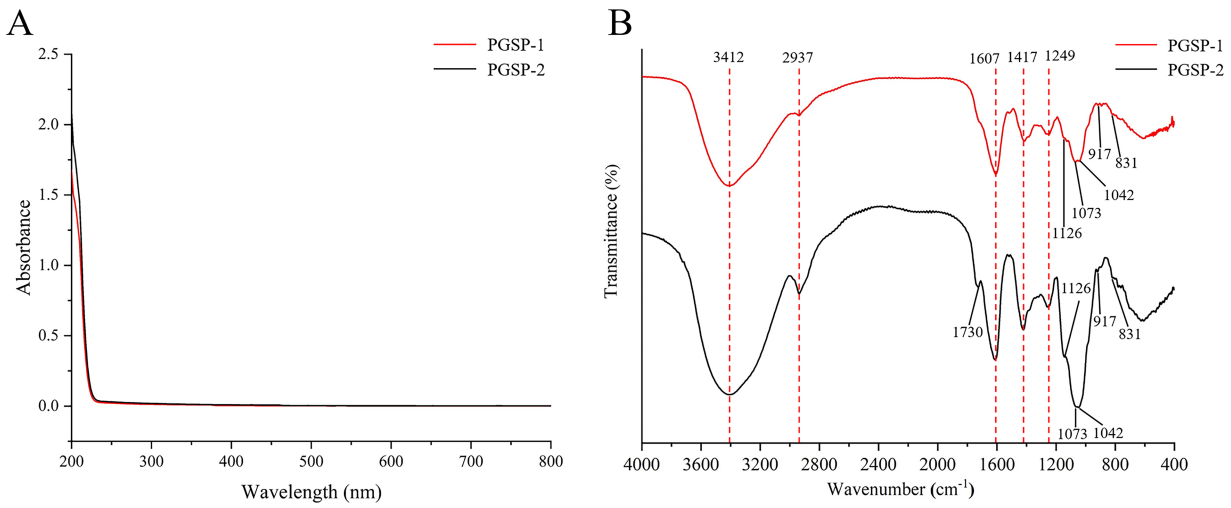

FIGURE 2
UV spectrum (A) and FT-IR spectrum (B) of PGSP-1 and PGSP-2.

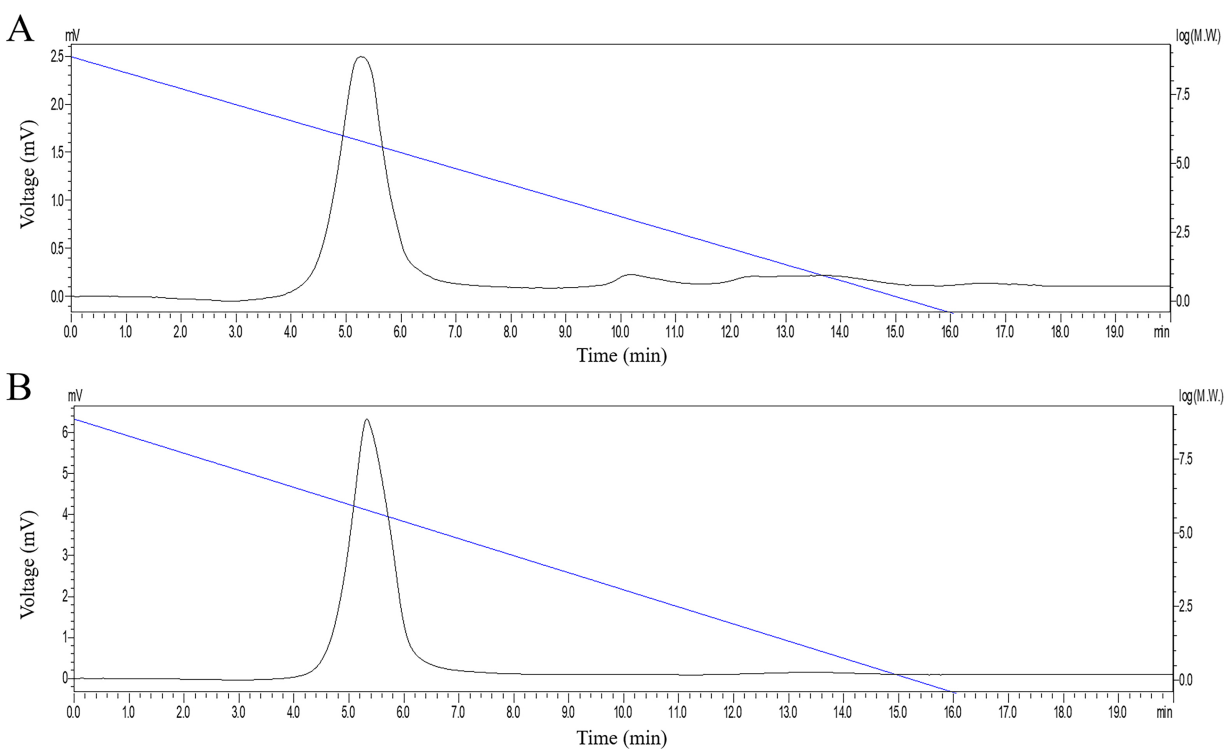

FIGURE 3
HPGPC profiles of PGSP-1 (A) and PGSP-2 (B).

of the dextran standard curve (logMw = − 0.58 T + 8.86), the molecular weights of PGSP-1 and PGSP-2 were calculated to be 723.83 and 620.48 kDa, respectively. The molecular weights of PGSP-1 and PGSP-2 both exceeded 50 kDa, indicating that they belonged to macromolecular polysaccharides (Ye, 2007). Furthermore, the distributive coefficients of PGSP-1 and PGSP-2 were 1.43 and 1.38 both closed to 1.0, demonstrating that the two were homogeneous polysaccharides (Fu, 2023).

3.2.4 Monosaccharide composition analysis

Based on the retention time of mixed standard substance, the monosaccharide compositions of PGSP-1 and PGSP-2 were determined. The HPLC chromatogram was shown in Figure 4, and PGSP-1 was consisted of Man, Rha, Glc, Gal and Ara in the molar ration of 2.04:3.53:1.00:7.82:1.70, as well as PGSP-2 was comprised of Man, Rha, GlcA, GalA, Glc, Gal, Xyl and Ara in the molar ration of 3.31:23.97:3.50:2.53:18.22:38.50:1.00:4.13. Compared to

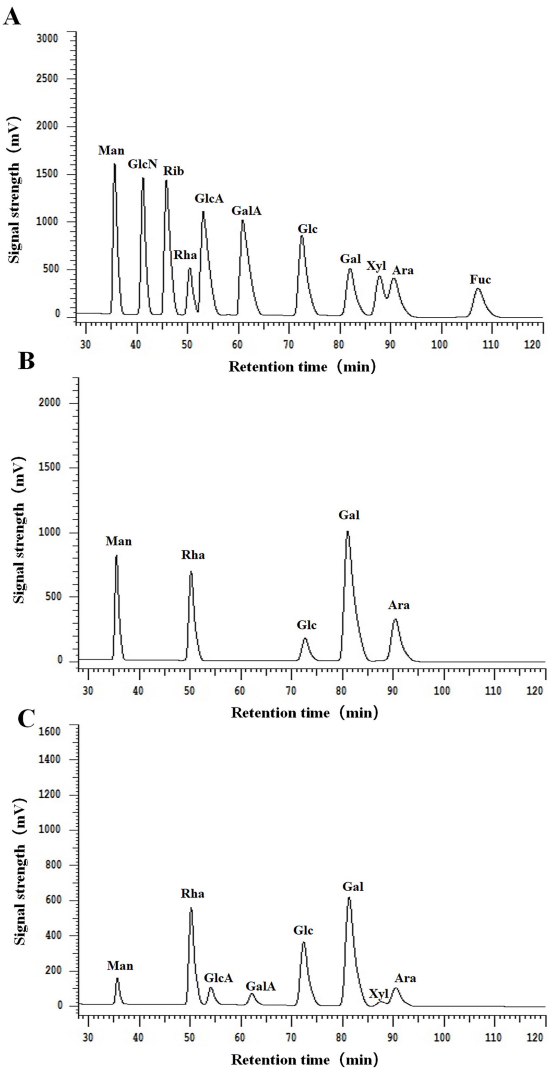

FIGURE 4
HPLC chromatograms of standard (A), PGSP-1 (B) and PGSP-2 (C).

PGSP-1, PGSP-2 also contained uronic acid and Xyl, which further verified PGSP-1 was neutral polysaccharide and PGSP-2 was acidic polysaccharide in the results of chemical composition analysis.

Kim et al. (2020) and Zhao et al. (2019) extracted WGNP, MPPG and WPPG from roots of *P. ginseng*, and Wang (2021) extracted GSLP-1, GSLP-2, GSLP-3, and GSLP-4 from stems and leaves of *P. ginseng*, and the results of monosaccharide composition showed that Glc accounted for the highest molar ratio. Tai et al. (1990) extracted SA1 from stems of *P. ginseng*, whose monosaccharide composition result showed that it was mainly conposed of Gal and Glc. Compared with the previous studies mentioned above, it was quite interesting that PGSP-1 and PGSP-2 from stems of *P. ginseng* were mainly consisted of Gal, which would make it showed alternative pharmacological activity.

3.2.5 SEM analysis

The morphology and microstructure of PGSP-1 and PGSP-2 was observed at the magnifications of 1.00, 5.00, and 15.00 k by SEM. As shown in Figure 5, PGSP-1 and PGSP-2 were both blocky, in which the surface of PGSP-1 was quite flat and covered a small amount of tiny particles, while the surface of PGSP-2 was relatively coarse and uneven with more tiny particles. Compared with PGSP-1, the surface of PGSP-2 was rougher and had some pores, providing more binding sites and interaction space for its combination with functional groups such as water molecules, which might improve the water solubility of polysaccharides and affect their pharmacological activity (Su, 2020).

3.2.6 TGA analysis

The thermal stability of PGSP-1 and PGSP-2 evaluated through TGA was demonstrated in Figure 6, in which there were two stages in the thermal weight loss process caused by the evaporation of bound water and the thermal degradation of polysaccharides (Kou et al., 2022; Shi et al., 2022). In the first stage, the DTG peak and mass loss rate were similar in PGSP-1 and PGSP-2. In the second stage, the DTG peak of PGSP-2 was slightly higher than PGSP-1, and the mass loss rate was significantly lower than PGSP-1, indicating that PGSP-2 had better thermal stability. The difference in stability between the two indicated the difference in structure, which might make it had different pharmacological activities.

3.2.7 Methylation analysis

To elucidate and evaluate structural characteristics of PGSP-1 and PGSP-2, the methylation analysis was carried out to determine glycosidic bond linkage patterns of them. As exhibited in Figure 7 and Table 1, the partially PMAAs of PGSP-1 were 2,3,5-Me_3-Ara*f*, 1,2,3,6-Me_4-Gal*p*, 3,4-Me_2-Rha*p*, 2,3,4-Me_3-Glc*p*, 2,3,6-Me_3-Gal*p*, 3,4-Me_2-Man*p* and 2,3-Me_2-Gal*p* which were corresponded to the glycosidic bonds of Ara*f*-(1→, →4)-Gal*p*, →2)-Rha*p*-(1→, →6)-Glc*p*-(1→, →4)-Gal*p*-(1→, →2,6)-Man*p*-(1→ and →4,6)-Gal*p*-(1→, at the molar percentages of 15.23, 8.51, 19.38, 11.16, 3.27, 20.14 and 22.31%. And there were more chromatogram peaks in total ion chromatogram (TIC) of PGSP-2, including 2,3,5-Me_3-Ara*f*, 2,3,4,6-Me_4-Glc*p*, 3,4-Me_2-Man*p*, 3,4-Me_2-Rha*p*, 2,3,4-Me_3-Glc*p*, 2,4,6-Me_3-Glc*p*, 2,3,6-Me_3-Gal*p*, 2,3-Me_2-Xyl*p* and 2,3-Me_2-Gal*p*. The glycosidic bonds corresponded to the PMAAs of PGSP-2 were Ara*f*-(1→, Glc*p*-(1→, →2,6)-Man*p*-(1→, →2)-Rha*p*-(1→, →6)-Glc*p*-(1→, →3)-Glc*p*-(1→, →4)-Gal*p*-(1→, →4)-Xyl*p*-(1→ and →4,6)-Gal*p*-(1→ at the molar percentages of 5.33, 3.48, 3.68, 26.83, 19.08, 3.09, 15.09, 1.05 and 22.37%. Additionally, the branching degrees of PGSP-1 and PGSP-2 were calcucated to be 0.66 and 0.35 using the method (Yang et al., 2010) as reported previously.

3.2.8 NMR analysis

As shown in Figures 8, 9 and Table 2, the characteristic structures of PGSP-1 and PGSP-2 were analyzed by means of 1D and 2D NMR, and the chemical shifts of PGSP-1 and PGSP-2 were assigned by referring to the chemical shifts reported in the relevant literature, so as to clarify the structures of PGSP-1 and PGSP-2. The ^{1}H NMR spectrum of PGSP-1 revealed that the hydrogen proton signals mainly concentrated in the 3.0–5.5 ppm region, and it was difficult to resolve because of more hydrogen and the close chemical shifts of polysaccharides (Guo et al., 2022). Most findings demonstrated that anomeric hydrogen proton signals of polysaccharides mainly dispersed from 4.3 to 5.5 ppm, in which the anomeric hydrogen proton signals of β-configuration usually appeared between 4.3 and 4.9 ppm, while the anomeric hydrogen proton signals of α-configuration were mostly concentrated in the

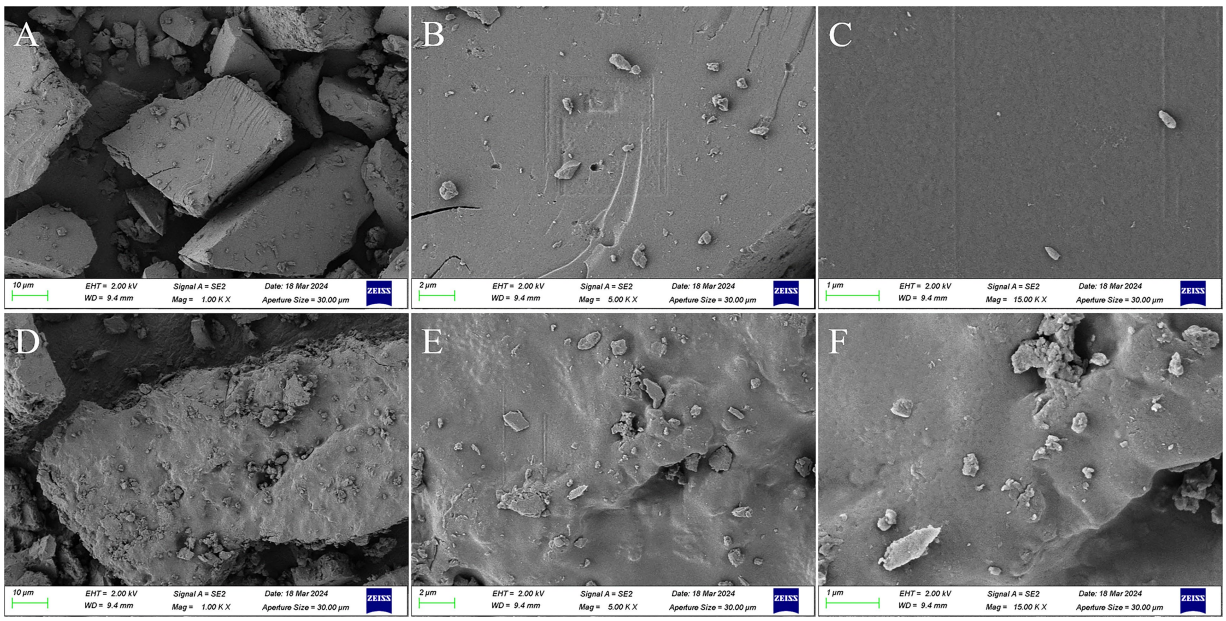

FIGURE 5
SEM images of PGSP-1 (A–C) and PGSP-2 (D–F).

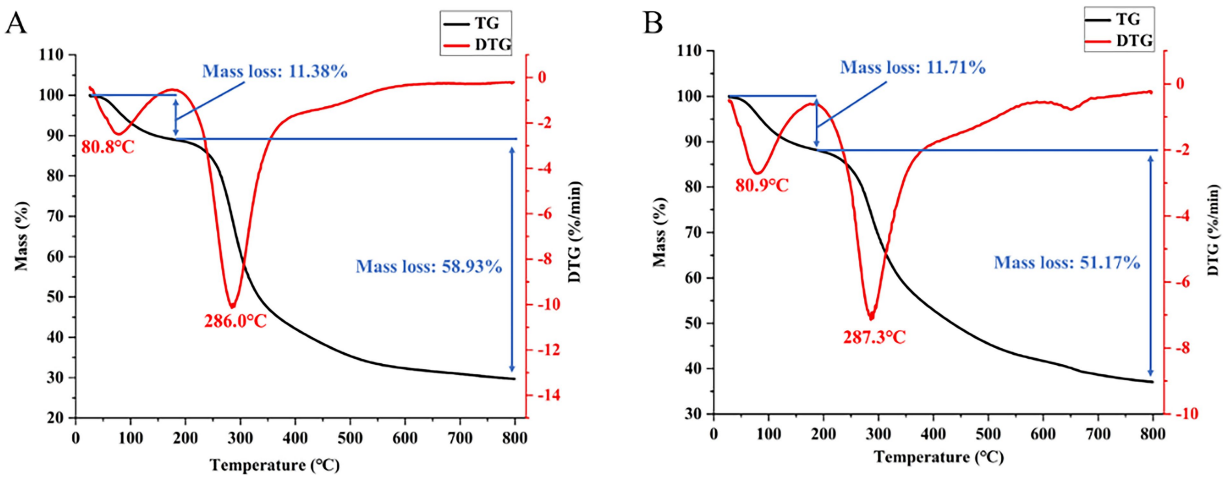

FIGURE 6
TG and DTG curves of PGSP-1 (A) and PGSP-2 (B).

range of 4.9–5.5 ppm (Peng et al., 2023). In the ^{1}H NMR spectrum of PGSP-1 (Figure 8A), it was evident that there were multiple hydrogen proton signals appearing in the range of 4.3–5.5 ppm of chemical shift, revealing that α-configuration and β-configuration both existed in PGSP-1. Additionally, there was an obvious signal peak showing up at the chemical shift of 1.24 ppm, which was attributed to the hydrogen proton signal on the methyl group, indicating the existence of rhamnose.

In ^{13}C NMR spectrum, the carbon signals of polysaccharides mainly concentrated in the region of 60–110 ppm, in which the chemical shifts of anomeric carbon signals mostly appeared within 90–110 ppm (Guo et al., 2022; Cui et al., 2023). In the ^{13}C NMR spectrum of PGSP-1 (Figure 8B), it was plain to observe that the chemical shifts of anomeric carbon signals were at 109.26, 104.28, 103.23, 100.39, 99.36, 98.37, and 96.73 ppm, indicating that there were seven glycosidic bonds in PGSP-1 and labeled them as A–G. In addition, the signal peak at the chemical shift of 16.55 ppm was caused by the carbon signal on the methyl group in rhamnose, which was corresponded with above-mentioned monosaccharide composition analysis and ^{1}H NMR spectrum of PGSP-1.

The HSQC NMR was carried out to determine the coupling relationship between carbon and its directly connected hydrogen in polysaccharides. In the HSQC spectrum of PGSP-1 (Figure 8C), the chemical shift of anomeric hydrogen proton signal in residue A was at 5.17 ppm, revealing that residue A was α-configuration. Based on the methylation analysis results and related literature, it was hypothesized

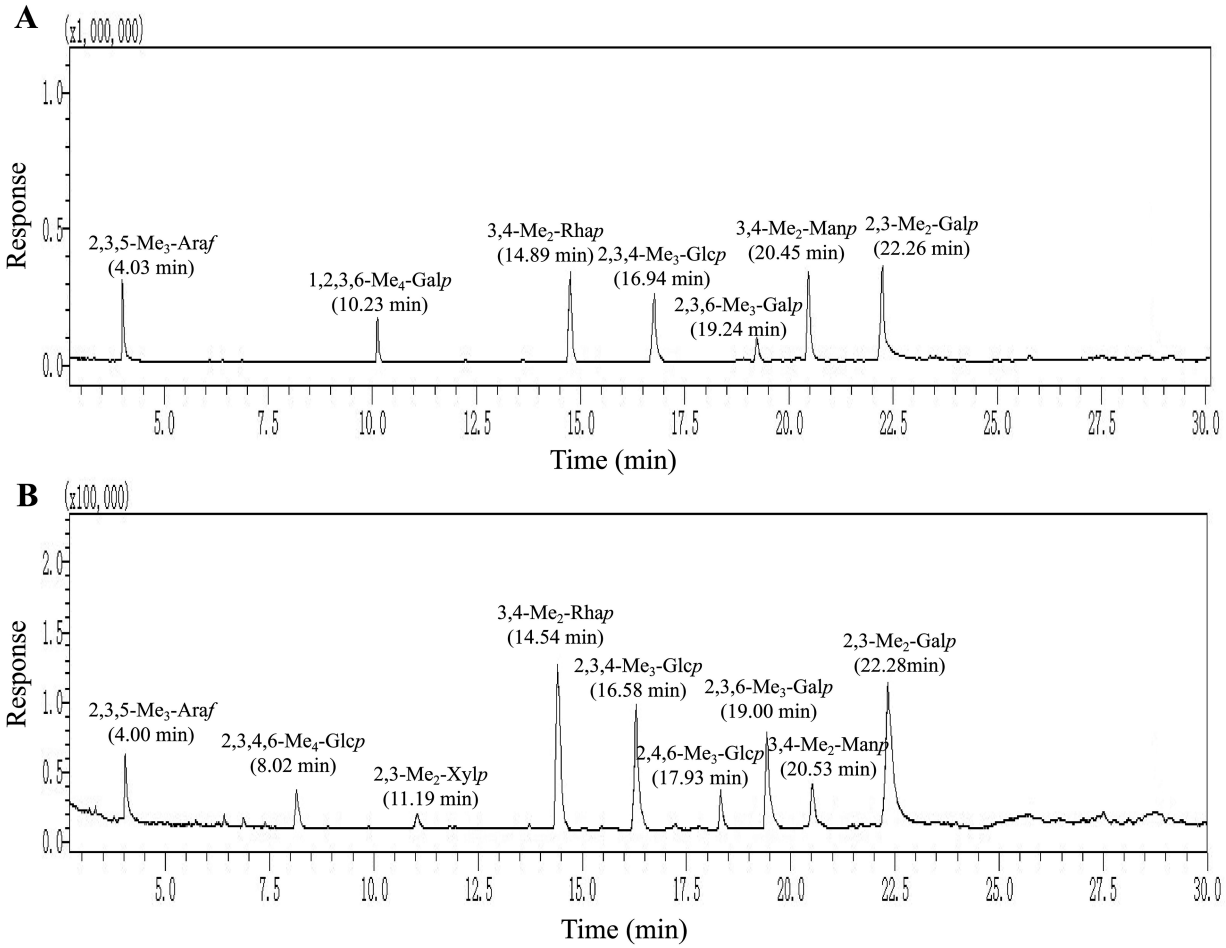

FIGURE 7
TIC of methylation products of PGSP-1 (A) and PGSP-2 (B).

that A was α-L-Ara*f*-(1→(Cui et al., 2023), and its associated δH2-5/C2-5 were 4.17/82.48, 3.86/76.53, 4.05/83.81 and 3.62/62.69. Likewise, B–G were speculated to be →4)-β-D-Gal*p*-(1→(Wu J. Y. et al., 2024), →4,6)-β-D-Gal*p*-(1→(Wu Z. W. et al., 2024), →6)-α-D-Glc*p*-(1→(Guo et al., 2022), →2)-α-L-Rha*p*-(1→(Zou et al., 2022), →2,6)-α-D-Man*p*-(1→(Tang et al., 2022) and →4)-β-D-Gal*p* (Wang et al., 2023).

Similarly, in the ^{1}H NMR spectrum of PGSP-2 (Figure 9A), there existed hydrogen proton signal peaks at 5.25, 5.15, 5.08, 5.02, 4.62, 4.56, 4.40, and 4.34 ppm in the range of 4.3–5.5 ppm of chemical shift, demonstrating that α-configuration and β-configuration both existed in PGSP-2.

In the ^{13}C NMR spectrum of PGSP-2 (Figure 9B), there were 10 anomeric carbon signal peaks at 109.26, 104.59, 104.19, 103.88, 103.40, 102.42, 100.15, 99.55, 98.60, and 97.95 ppm and marked them as A'–J'. It was obvious to demonstrate that PGSP-2 possessed 10 glycosidic bonds, while only eight anomeric hydrogen proton signal peaks existed in the ^{1}H NMR spectrum of PGSP-2. It might be due to the fact that the chemical shifts of some hydrogen protons were very similar, the signal peaks overlapped, and the signal peaks appearing at the chemical shift of 4.62–5.01 ppm might be covered by the solvent peak. In particular, it was noteworthy that there were two signal peaks at 174.75 and 175.10 ppm, attributed to the carboxyl carbon on the uronic acid in PGSP-2, which was consistent with the analysis results of monosaccharide composition and characteristic groups.

In the HSQC spectrum of PGSP-2 (Figure 9C), PGSP-2 was analyzed using the identical method and the analysis revealed that in addition to the six same glycosidic bonds with PGSP-1, PGSP-2 also had four different cross peaks at 4.40/104.59, 4.62/103.88, 4.75/102.42, and 5.08/97.95 ppm, and the corresponding glycosidic bonds were speculated to be →4)-β-D-Xyl*p*-(1→(Huang et al., 2023), →4)-β-D-Gal*p*A-(1→(Ji et al., 2020), →3)-β-D-Glc*p*A-(1→(Huo et al., 2020) and α-D-Glc*p*-(1→(Wang J. Y. et al., 2024). As presented in Table 2, the ^{1}H and ^{13}C NMR chemical shifts of PGSP-1 and PGSP-2 were assigned by combining the above data analysis and referring to the relevant literature.

3.3 Hypoglycemic activity analysis of PGSPs *in vitro*

3.3.1 α-glycosidase and α-amylase inhibitory activity of PGSPs

To futher evalued polysaccharides on hypoglycemic activities *in vitro*, α-glycosidase and α-amylase inhibition assays would be taken into consideration firstly for the fact that α-glycosidase and α-amylase

10.3389/fsufs.2024.1500278

TABLE 1 The methylation results of PGSP-1 and PGSP-2.

Methylated sugars	Type of linkage	Molar ration (%)	Mass fragments (m/z)
PGSP-1			
2,3,5-Me_3-Ara*f*	Ara*f*-(1→	15.23	43, 57, 61, 70, 73, 86, 98, 103, 116, 145
1,2,3,6-Me_4-Gal*p*	→4)-Gal*p*	8.51	32, 41, 43, 55, 57, 69, 71, 85, 99, 113, 127
3,4-Me_2-Rha*p*	→2)-Rha*p*-(1→	19.38	32, 43, 62, 72, 82, 96, 103, 112, 145, 172
2,3,4-Me_3-Glc*p*	→6)-Glc*p*-(1→	11.16	32, 43, 71, 87, 101, 117, 129, 145, 161, 205
2,3,6-Me_3-Gal*p*	→4)-Gal*p*-(1→	3.27	41, 43, 57, 71, 87, 101, 117, 129, 143, 161, 173, 233
3,4-Me_2-Man*p*	→2,6)-Man*p*-(1→	20.14	32, 43, 55, 69, 71, 85, 99, 113, 117, 129
2,3-Me_2-Gal*p*	→4,6)-Gal*p*-(1→	22.31	43, 57, 73, 85, 97, 113, 129, 141, 159, 171, 185, 199, 213, 227, 256
PGSP-2			
2,3,5-Me_3-Ara*f*	Ara*f*-(1→	5.33	42, 43, 56, 61, 70, 73, 84, 86, 98, 103, 116, 145
2,3,4,6-Me_4-Glc*p*	Glc*p*-(1→	3.48	32, 43, 55, 71, 85, 87, 101, 117, 129, 131, 145, 161, 205
2,3-Me_2-Xyl*p*	→4)-Xyl*p*-(1→	1.05	43, 57, 85, 103, 115, 145, 170, 187, 217, 259, 289, 361
3,4-Me_2-Rha*p*	→2)-Rha*p*-(1→	26.83	32, 43, 61, 72, 82, 96, 103, 112, 142, 159, 172
2,3,4-Me_3-Glc*p*	→6)-Glc*p*-(1→	19.08	32, 40, 43, 55, 57, 69, 71, 85, 99, 113, 127
2,4,6-Me_3-Glc*p*	→3)-Glc*p*-(1→	3.09	32, 43, 55, 71, 85, 101, 117, 129, 145, 161
2,3,6-Me_3-Gal*p*	→4)-Gal*p*-(1→	15.09	41, 43, 57, 71, 87, 99, 117, 129, 142, 161, 173, 233
3,4-Me_2-Man*p*	→2,6)-Man*p*-(1→	3.68	32, 43, 48, 71, 89, 99, 117, 131, 189
2,3-Me_2-Gal*p*	→4,6)-Gal*p*-(1→	22.37	41, 43, 78, 85, 97, 115, 129, 143, 157, 171, 185, 199, 213, 227, 239, 256

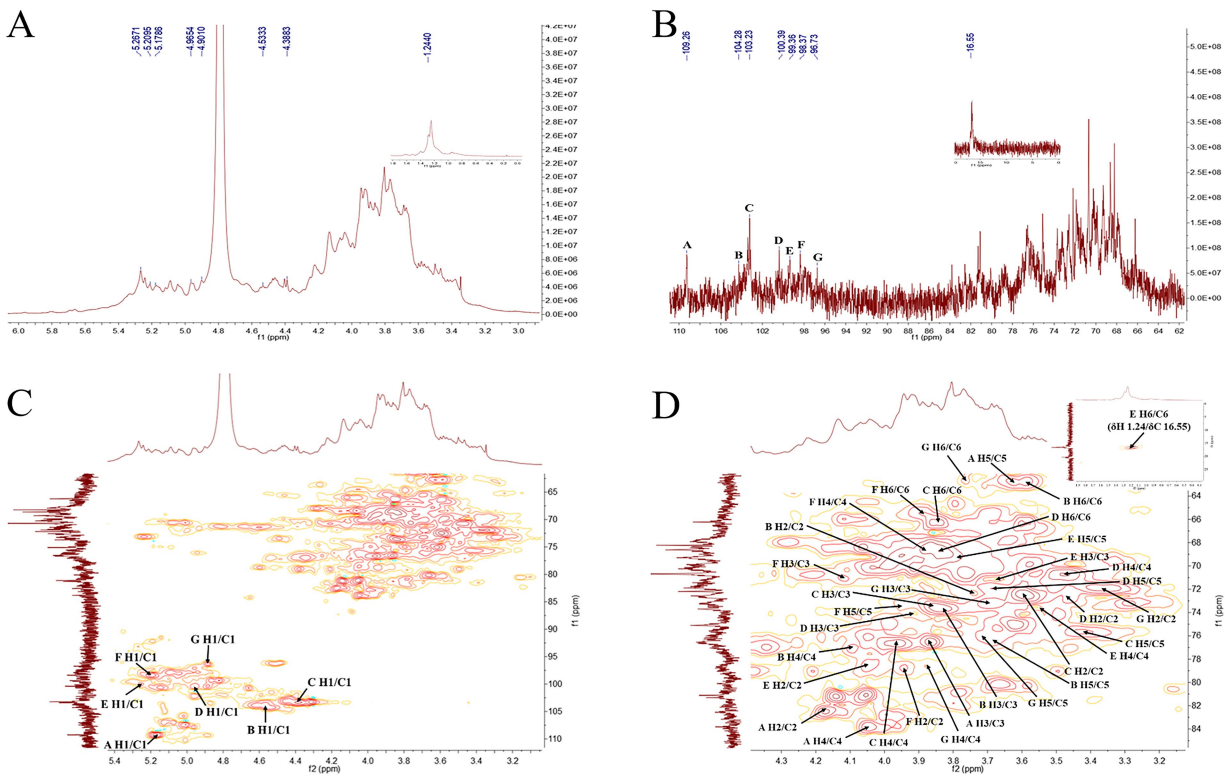

FIGURE 8
^{1}H NMR (A), ^{13}C NMR (B), HSQC (C) and partial enlarged diagram of δH2-6/C2-6 (D) spectra of PGSP-1.

were the key enzymes in the process of carbohydrate digestion and absorption into blood glucose, which led to the increase of blood glucose (An et al., 2022). As shown in Figure 10, PGSP-1 and PGSP-2 showed dose-dependent inhibitory effects on α-glycosidase and α-amylase in the range of 0.2–1.0 mg/mL, and reached the maximum inhibition rate at 1.0 mg/mL. The reason why the inhibition rate of

10.3389/fsufs.2024.1500278

TABLE 2 Chemical shift assignments of the PGSP-1 and PGSP-2.

Glycosyl residues		Chemical shifts (ppm)					
		H1/C1	H2/C2	H3/C3	H4/C4	H5/C5	H6/C6
PGSP-1							
A	α-L-Araf-(1→	5.17/109.26	4.17/82.48	3.86/76.53	4.05/83.81	3.62/62.69	—
B	→4)-β-D-Galp-(1→	4.53/104.28	3.74/72.44	3.84/73.62	4.09/77.12	3.68/76.19	3.59/62.75
C	→4,6)-β-D-Galp-(1→	4.38/103.23	3.60/72.43	3.86/73.51	3.97/76.64	3.43/75.69	3.84/66.29
D	→6)-α-D-Glcp-(1→	4.96/100.39	3.46/72.51	3.91/74.05	3.47/70.73	3.69/72.07	3.84/68.82
E	→2)-α-L-Rhap-(1→	5.26/99.36	4.05/78.64	3.67/71.18	3.56/73.62	3.74/69.11	1.24/16.55
F	→2,6)-α-D-Manp-(1→	5.20/98.37	3.94/78.77	4.12/71.09	3.87/68.56	3.95/73.70	3.89/65.47
G	→4)-β-D-Galp	4.90/96.73	3.38/72.86	3.70/73.32	3.89/78.60	3.71/76.31	3.76/62.69
PGSP-2							
A’	α-L-Araf-(1→	5.15/109.26	4.23/82.43	3.86/76.49	4.05/83.81	3.65/62.74	—
B′	→4)-β-D-Xylp-(1→	4.40/104.59	3.61/75.04	4.03/76.11	4.01/77.02	4.06/66.19	—
C′	→4)-β-D-Galp-(1→	4.56/104.19	3.69/72.97	3.81/73.57	4.08/77.18	3.68/76.38	3.56/62.55
D′	→4)-β-D-GalpA-(1→	4.62/103.88	3.82/72.87	3.94/73.29	4.13/81.25	4.35/76.97	–/174.75
E’	→4,6)-β-D-Galp-(1→	4.34/103.40	3.58/72.60	3.82/73.48	3.95/77.03	3.40/75.70	3.83/66.40
F′	→3)-β-D-GlcpA-(1→	4.75/102.42	3.28/73.35	3.80/78.21	4.02/70.26	4.12/73.48	–/175.10
G’	→6)-α-D-Glcp-(1→	5.02/100.15	3.37/72.83	3.91/73.87	3.28/70.85	3.69/72.17	3.82/68.57
H′	→2)-α-L-Rhap-(1→	5.25/99.65	4.16/78.63	3.68/71.19	3.48/73.54	3.70/69.07	1.24/16.54
I′	→2,6)-α-D-Manp-(1→	5.17/98.60	4.03/78.84	4.15/71.04	3.82/68.08	3.88/73.16	3.87/65.10
J’	α-D-Glcp-(1→	5.08/97.95	3.31/72.72	3.37/73.37	3.58/70.31	3.92/72.09	3.70/62.69

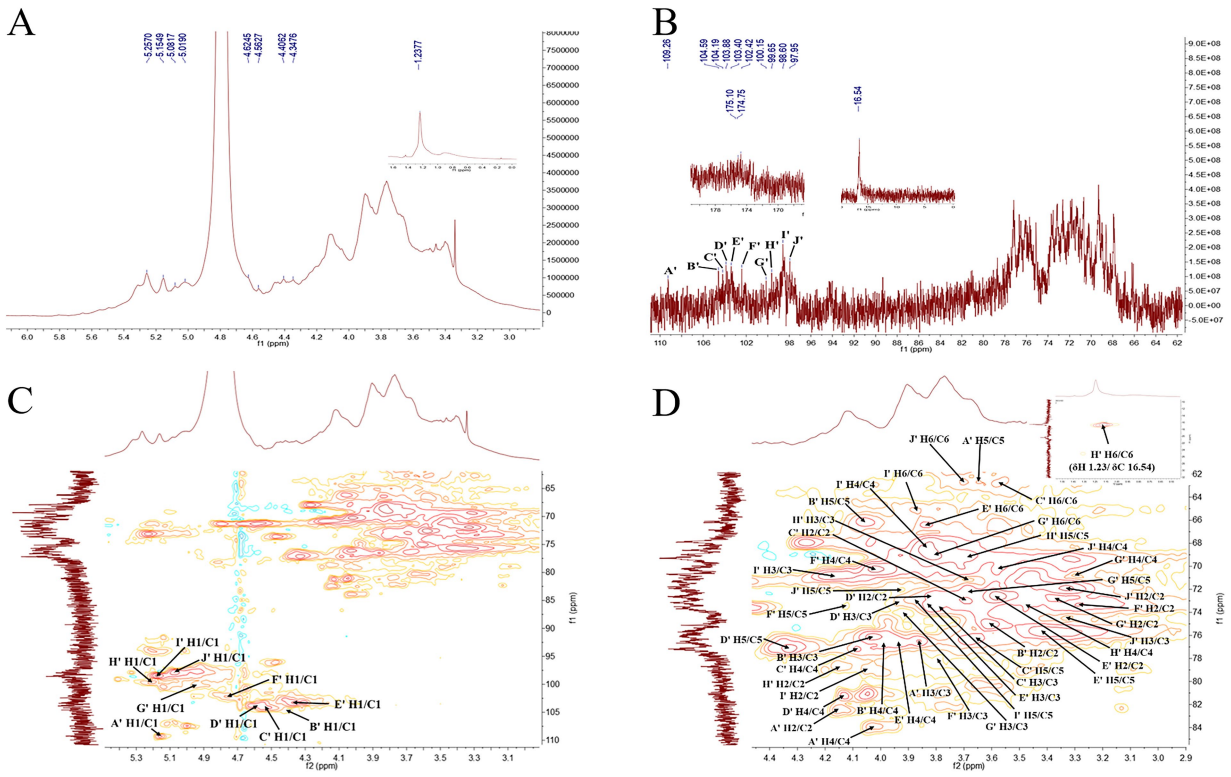

FIGURE 9
^{1}H NMR (A), ^{13}C NMR (B), HSQC (C) and partial enlarged diagram of δH2-6/C2-6 (D) spectra of PGSP-2.

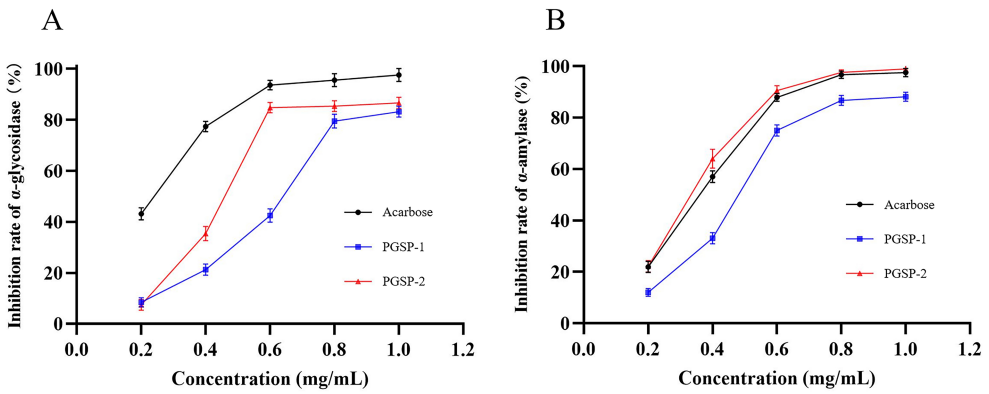

FIGURE 10
Inhibitory effects of PGSP-1 and PGSP-2 on α-glycosidase (A), α-amylase activity (B).

PGSP-1 and PGSP-2 on α-glycosidase and α-amylase increased constantly with the increase of the concentration of them was that the carboxylate and hydroxyl groups in PGSP-1 and PGSP-2 interacted with α-glycosidase and α-amylase, and the binding effect changed the polarity and molecular conformation of the enzyme, which eventually led to the loss of enzyme activity (Naveen and Baskaran, 2018; Dong et al., 2023). The IC_{50} values of PGSP-1, PGSP-2 and acarbose were calculated to be 0.61 ± 0.026, 0.45 ± 0.030 and 0.28 ± 0.024 mg/mL for α-glycosidase, and 0.46 ± 0.027, 0.31 ± 0.028 and 0.34 ± 0.031 mg/mL for α-amylase, respectively. These findings demonstrated that PGSP-2 always exhibited better performance whether on α-glycosidase or α-amylase and it was noteworthy that the inhibitory activity of PGSP-2 on α-amylase was even better than that of the positive control acarbose. And in previous study, Yang et al. (1991) studied hypoglycemic activity of *P. ginseng* stems and leaves polysaccharides *in vivo* and found that polysaccharides could effectively inhibit the increase of blood glucose in rats, indicating that polysaccharides of *P. ginseng* stems and *P. ginseng* stems and leaves had hypoglycemic activity preliminarily.

The hypoglycemic activity of polysaccharides was closely related to their molecular weight, monosaccharide composition, uronic acid content and glycosyl linkage types (An et al., 2022; Chen X. X. et al., 2023). Based on a previous study, Xu et al. (2018) found that the polysaccharide fractions from blackcurrant fruits with the lowest molecular weight presented the highest inhibitory effects on α-glycosidase and α-amylase. Seedevi et al. (2020) revealed that rhamnose-enriched polysaccharides had the effect on reversing the blood glucose concentration. Li et al. (2017) reported that uronic acid polysaccharides from yams with the highest uronic acid content had the best hypoglycemic effect. Dong et al. (2023) had shown that the presence β-D linked Gal might affect the mechanism of inhibition of digestive enzymes such as α-glycosidase and α-amylase. In summary, PGSP-2 had lower molecular weight, more abundant rhamnose, higher proportion of effective monosaccharides and more uronic acid content compared to PGSP-1, affecting that it had better performance on the inhibitory activity of α-glycosidase and α-amylase.

3.3.2 Inhibitory kinetics of PGSPs on α-glycosidase and α-amylase

The double-reciprocal Lineweaver-Burk plots were performed to determinate the relation between V and the concentration of polysaccharide at 0, 0.2, 0.4 and 0.8 mg/mL, in which X-axis, Y-axis, horizontal axis intercept, vertical axis intercept and slope represented reciprocal of different concentrations of the substrate, 1/V, absolute value of 1/Km,1/Vmax and Km/Vmax, respectively. The inhibition kinetics of PGSP-1 and PGSP-2 on α-glycosidase and α-amylase was shown in Figure 11 and Table 3. As shown in Figure 11A, all the straight lines intersected on the X axis, and with the increase of substrate concentration, the value of Vmax decreased and Km value remained unchanged, indicating that inhibition of PGSP-1 against α-glycosidase was non-competitive type inhibition. When all the straight lines intersected in the second or third quadrant, and with the increase of substrate concentration, the value of Vmax decreased and Km value increased, indicating that the inhibition of PGSPs on α-glycosidase and α-amylase was mixed type inhibition (Pan et al., 2023; Gu et al., 2021). The results in Figures 11B–D demonstrated that the inhibition of PGSP-1 on α-amylase and PGSP-2 on both α-glycosidase and α-amylase was mixed type inhibition. Compared to previous studies, it showed a huge difference from PGSPs that the inhibition kinetics of polysaccharides from sweet corncob (Wang et al., 2023) and blue honeysuckle berries (Fu et al., 2020) against α-glycosidase and α-amylase was competitive type inhibition, in which the possible reason was that the difference between the structure of PGSPs determined the difference in binding to the enzymes, affecting the inhibition of PGSPs against α-glycosidase and α-amylase.

4 Conclusion

In this study, two novel polysaccharides (PGSP-1 and PGSP-2) with hypoglycemic activity obtained from *P. ginseng* stems for the first time were studied in detail and reported systematically. The structural characterization results demonstrated that PGSP-1 (Mw = 723.83 kDa) and PGSP-2 (Mw = 620.48 kDa) were characterized →4)-β-D-Gal*p*-(1→, →6)-α-D-Glc*p*-(1→ and →2)-α-L-Rha*p*-(1→ as the skeleton, →4,6)-β-D-Gal*p*-(1→ and →2,6)-α-D-Man*p*-(1→ as the cross junction, α-L-Araf-(1→ as the terminal unit, with different microstructures and thermal stability. And the hypoglycemic activity result revealed that PGSP-1 and PGSP-2 both showed excellent inhibitory activity against α-glucosidase and α-amylase, in which

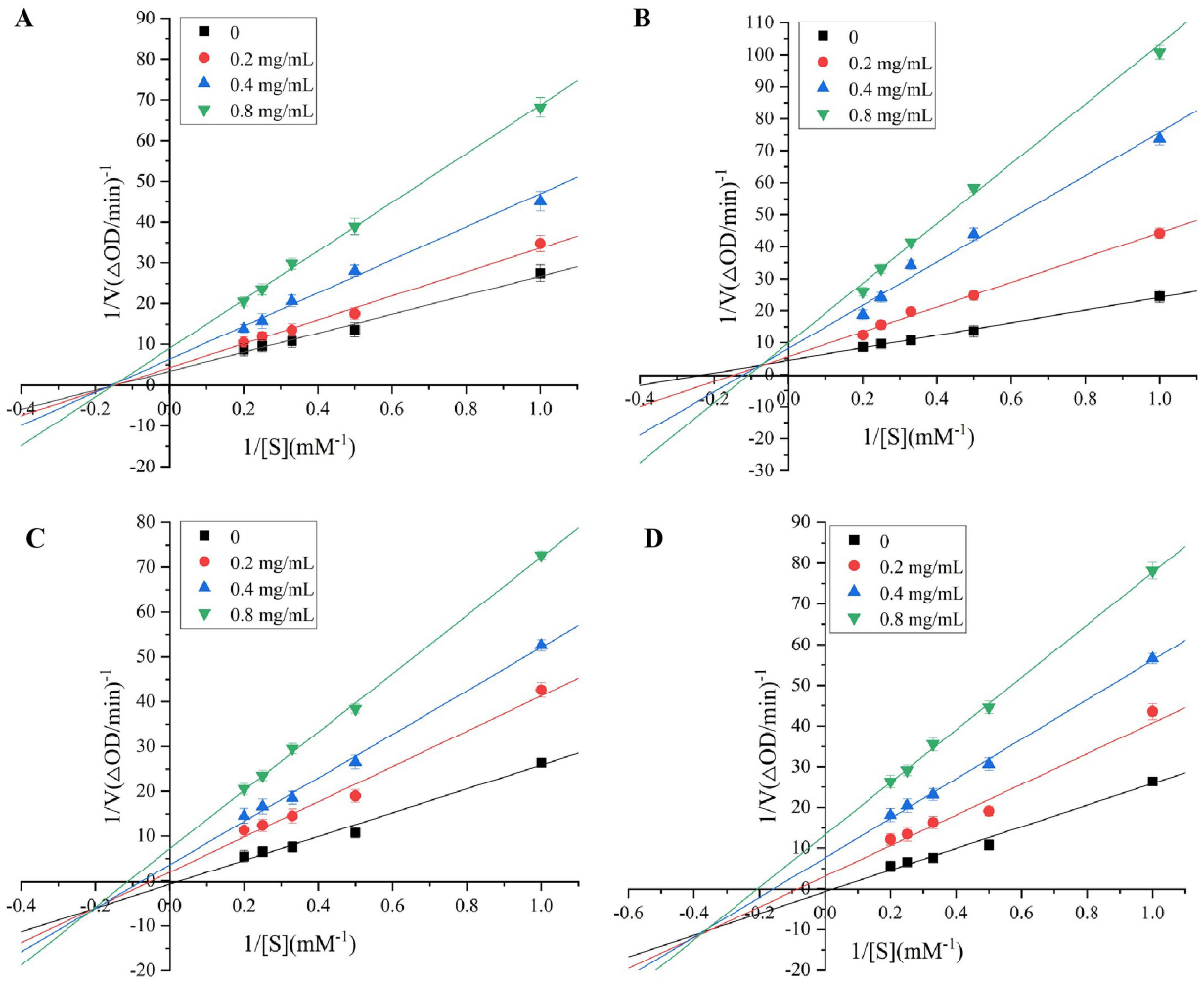

FIGURE 11
Lineweaver-Burk plots for inhibition of α-glucosidase by PGSP-1 (A) and PGSP-2 (B); Lineweaver-Burk plots for inhibition of α-amylase by PGSP-1 (C) and PGSP-2 (D).

TABLE 3 Kinetic parameters, Km, Vmax of PGSP-1 and PGSP-2 inhibiting α-glucosidase and α-amylase.

Enzyme	Samples	Concentration (mg/mL)	Km (mM)	Vmax (△OD/min)	Type of inhibition
α-Glucosidase	Blank	0	6.849	0.318	
	PGSP-1	0.2	6.896	0.234	Non-competitive
		0.4	6.395	0.157	
		0.8	6.666	0.111	
	PGSP-2	0.2	6.944	0.178	Mixed inhibition
		0.4	9.333	0.122	
		0.8	9.523	0.101	
α-Amylase	Blank	0	36.496	1.369	
	PGSP-1	0.2	20.408	0.518	Mixed inhibition
		0.4	13.531	0.278	
		0.8	9.041	0.138	
	PGSP-2	0.2	12.315	0.326	Mixed inhibition
		0.4	6.402	0.131	
		0.8	4.866	0.075	

PGSP-2 had the better performance. However, there are still some limitations in this study, more profound hypoglycemic activity experiments on cells *in vitro* need to be carried out in order to explore the potential hypoglycemic mechanism of PGSPs. This study provides sufficient theoretical support for effective development and utilization of PGSPs as healthy products with hypoglycemic activity and also provides new insight for the development of potential medicinal value from agro-byproducts that are about to be wasted, which will help attract more and more people to pay attention to the medicinal value and economic value of agro-byproducts such as *P. ginseng* stems in the future.

Data availability statement

The original contributions presented in the study are included in the article/supplementary material, further inquiries can be directed to the corresponding authors.

Author contributions

WX: Methodology, Writing – original draft. WZ: Investigation, Supervision, Visualization, Writing – review & editing. JS: Conceptualization, Project administration, Visualization, Writing – review & editing. WC: Software, Writing – original draft. XW: Formal Analysis, Writing – original draft. TG: Validation, Writing – original draft. YZ: Validation, Writing – original draft. PY: Formal analysis, Writing – original draft. ZH: Conceptualization, Data curation, Supervision, Writing – review & editing. GL: Supervision, Validation, Writing – review & editing.

Funding

The author(s) declare that financial support was received for the research, authorship, and/or publication of this article. This work was supported by the grant from the National Natural Science Foundation of China (Grant nos. 82360683 and 82360805), Jilin Provincial Science and Technology Department (Grant no. 20230508170RC), and Yanbian University Doctoral Initiation Fund Project (Grant no. ydbq202428).

Conflict of interest

The authors declare that the research was conducted in the absence of any commercial or financial relationships that could be construed as a potential conflict of interest.

Publisher's note

References

Alboofetileh, M., Rezaei, M., Tabarsa, M., Rittà, M., Donalisio, M., Mariatti, F., et al. (2019). Effect of different non-conventional extraction methods on the antibacterial and antiviral activity of fucoidans extracted from *Nizamuddinia zanardinii*. *Int. J. Biol. Macromol.* 124, 131–137. doi: 10.1016/j.ijbiomac.2018.11.201

An, K. J., Wu, J. J., Xiao, H. W., Hu, T. G., Yu, Y. S., Yang, W. Y., et al. (2022). Effect of various drying methods on the physicochemical characterizations, antioxidant activities and hypoglycemic activities of lychee (*Litchi chinensis* Sonn.) pulp polysaccharides. *Int. J. Biol. Macromol.* 220, 510–519. doi: 10.1016/j.ijbiomac.2022.08.083

Arab, K., Ghanbarzadeh, B., Ayaseh, A., and Jahanbin, K. (2021). Extraction, purification, physicochemical properties and antioxidant activity of a new polysaccharide from *Ocimum album* L. seed. *Int. J. Biol. Macromol.* 180, 643–653. doi: 10.1016/j.ijbiomac.2021.03.088

Bai, Y. Z. (2023). Extraction, purification, physicochemical properties, and hypoglycemic activity evaluation of Polysaccharides from Gynura divaricata (L.) DC. [Dissertation/Master's thesis]. Zhejiang Gongshang University.

Blumenkrantz, N., and Asboe-Hansen, G. (1973). New method for quantitative determination of uronic acids. *Anal. Biochem.* 54, 484–489. doi: 10.1016/0003-2697(73)90377-1

Bradford, M. M. (1976). A rapid and sensitive method for the quantitation of microgram quantities of protein utilizing the principle of protein-dye binding. *Anal. Biochem.* 72, 248–254. doi: 10.1016/0003-2697(76)90527-3

Cai, Y., Si, Z. Y., Jiang, Y., Ye, M., Wang, F., Yang, X. B., et al. (2023). Structure-activity relationship of low molecular weight *Astragalus membranaceus* polysaccharides produced by Bacteroides. *Carbohydr. Polym.* 316:121036. doi: 10.1016/j.carbpol.2023.121036

Chen, F., and Huang, G. L. (2019). Antioxidant activity of polysaccharides from different sources of ginseng. *Int. J. Biol. Macromol.* 125, 906–908. doi: 10.1016/j.ijbiomac.2018.12.134

Chen, J. C., Li, L., Zhang, X., Zhang, Y., Zheng, Q. S., Lan, M. J., et al. (2023). Structural characteristics and antioxidant and hypoglycemic activities of a heteropolysaccharide from *Anemarrhena asphodeloides* Bunge. *Int. J. Biol. Macromol.* 236:123843. doi: 10.1016/j.ijbiomac.2023.123843

Chen, Z. H., Wang, C. J., Su, J. R., Liang, G. X., Tan, S. F., Bi, Y. G., et al. (2024). Extraction of *Pithecellobium clypearia* Benth polysaccharides by dual-frequency ultrasound-assisted extraction: structural characterization, antioxidant, hypoglycemic and anti-hyperlipidemic activities. *Ultrason. Sonochem.* 107:106918. doi: 10.1016/j.ultsonch.2024.106918

Chen, X. X., Wu, J. L., Fu, X., Wang, P. P., and Chen, C. (2023). *Fructus mori* polysaccharide alleviates diabetic symptoms by regulating intestinal microbiota and intestinal barrier against TLR4/NF-κB pathway. *Int. J. Biol. Macromol.* 249:126038. doi: 10.1016/j.ijbiomac.2023.126038

Cui, Y. L., Chen, Y. J., Wang, S., Wang, S. X., Yang, J., Ismael, M., et al. (2023). Purification, structural characterization and antioxidant activities of two neutral polysaccharides from persimmon peel. *Int. J. Biol. Macromol.* 225, 241–254. doi: 10.1016/j.ijbiomac.2022.10.257

Dong, Y. H., Wang, Z. X., Chen, C., Wang, P. P., and Fu, X. (2023). A review on the hypoglycemic effect, mechanism and application development of natural dietary polysaccharides. *Int. J. Biol. Macromol.* 253:127267. doi: 10.1016/j.ijbiomac.2023.127267

Faidi, A., Becheikh, M. E. H., Lassoued, M. A., Safta, F., and Sfar, S. (2025). Isolation of sodium alginate-like polysaccharide from *Padina pavonica*: optimization, characterization and antioxidant properties. *J. Mol. Struct.* 1321:139737. doi: 10.1016/j.molstruc.2024.139737

Fu, J. (2023). Study on structural characterization, *in vitro* digestion and fermentation characteristics of Schisandrae Chinensis Fructus polysaccharides and its mechanism of improving Alzheimer's disease. [Dissertation/Master's thesis]. Changchun: Jilin University.

Fu, X. T., Yang, H. H., Ma, C. L., Li, X. Q., Li, D. L., Yang, Y., et al. (2020). Characterization and inhibitory activities on α-amylase and α-glucosidase of the polysaccharide from blue honeysuckle berries. *Int. J. Biol. Macromol.* 163, 414–422. doi: 10.1016/j.ijbiomac.2020.06.267

Ghamgui, H., Jarboui, R., Jeddou, K. B., Torchi, A., Siala, M., Cherif, S., et al. (2024). Polysaccharide from *Thymelaea hirsuta* L. leaves: structural characterization, functional properties and antioxidant evaluation. *Int. J. Biol. Macromol.* 262:129244. doi: 10.1016/j.ijbiomac.2024.129244

Ghosh, S., and Abdullah, M. F. (2024). Extraction of polysaccharide fraction from cadamba (*Neolamarckia cadamba*) fruits and evaluation of its *in vitro* and *in vivo* antioxidant activities. *Int. J. Biol. Macromol.* 279:135564. doi: 10.1016/j.ijbiomac.2024.135564

Gu, S. S., Sun, H. Q., Zhang, X. L., Huang, F. N., Pan, L. C., and Zhu, Z. Y. (2021). Structural characterization and inhibitions on α-glucosidase and α-amylase of alkali-extracted water-soluble polysaccharide from *Annona squamosa* residue. *Int. J. Biol. Macromol.* 166, 730–740. doi: 10.1016/j.ijbiomac.2020.10.230

Guo, M. K., Shao, S., Wang, D. D., Zhao, D. Q., and Wang, M. X. (2021). Recent progress in polysaccharides from *Panax ginseng* CA Meyer. *Food Funct.* 12, 494–518. doi: 10.1039/d0fo01896a

Guo, Y. D., Wang, L. L., Li, L., Zhang, Z. Y., Zhang, J. Q., Zhang, J., et al. (2022). Characterization of polysaccharide fractions from *Allii macrostemonis* bulbus and assessment of their antioxidant. *Lwt.* 165:113687. doi: 10.1016/j.lwt.2022.113687

Guo, D. Q., Yin, X. X., Wu, D. M., Chen, J. L., and Ye, X. Q. (2023). Natural polysaccharides from *Glycyrrhiza uralensis* residues with typical glucan structure showing inhibition on α-glucosidase activities. *Int. J. Biol. Macromol.* 224, 776–785. doi: 10.1016/j.ijbiomac.2022.10.165

Han, H. M., Zhang, H. X., Wang, Z. Y., Song, Y. J., Zhou, H. L., and Qu, X. S. (2024). Rapidly identification of ginseng from different origins using three-step infrared macro-fingerprinting technique. *J. Mol. Struct.* 1310:138332. doi: 10.1016/j.molstruc.2024.138332

Hong, T., Yin, J. Y., Nie, S. P., and Xie, M. Y. (2021). Applications of infrared spectroscopy in polysaccharide structural analysis: progress, challenge and perspective. *Food Chemistry: X.* 12:100168. doi: 10.1016/j.fochx.2021.100168

Hu, X. T., Xu, F. R., Li, J. L., Li, J., Mo, C., Zhao, M., et al. (2022). Ultrasonic-assisted extraction of polysaccharides from coix seeds: optimization, purification, and *in vitro* digestibility. *Food Chem.* 374:131636. doi: 10.1016/j.foodchem.2021.131636

Huang, X. Z., Wen, Y. X., Chen, Y. H., Liu, Y. Y., and Zhao, C. (2023). Structural characterization of *Euglena gracilis* polysaccharide and its *in vitro* hypoglycemic effects by alleviating insulin resistance. *Int. J. Biol. Macromol.* 236:123984. doi: 10.1016/j.ijbiomac.2023.123984

Huo, J. Y., Lu, Y., Jiao, Y. K., and Chen, D. F. (2020). Structural characterization and anticomplement activity of an acidic polysaccharide from *Hedyotis diffusa*. *Int. J. Biol. Macromol.* 155, 1553–1560. doi: 10.1016/j.ijbiomac.2019.11.132

Ji, X. L., Yan, Y. Z., Hou, C. Y., Shi, M. M., and Liu, Y. Q. (2020). Structural characterization of a galacturonic acid-rich polysaccharide from *Ziziphus Jujuba* cv, Muzao. *Int. J. Biol. Macromol.* 147, 844–852. doi: 10.1016/j.ijbiomac.2019.09.244

Jiang, Q. H., Chen, L., Wang, R., Chen, Y., Deng, S. G., Shen, G. X., et al. (2024). Hypoglycemic mechanism of *Tegillarca granosa* polysaccharides on type 2 diabetic mice by altering gut microbiota and regulating the PI3K-akt signaling pathway. *Food Sci. Human Wellness* 13, 842–855. doi: 10.26599/FSHW.2022.9250072

Kim, H. M., Song, Y. X., Hyun, G. H., Long, N. P., Park, J. H., Hsieh, Y. S., et al. (2020). Characterization and antioxidant activity determination of neutral and acidic polysaccharides from *Panax Ginseng* C. A. Meyer. *Molecules* 25:791. doi: 10.3390/molecules25040791

Kou, R. B., Zuo, G. L., Liu, J. F., Di, D. L., and Guo, M. (2022). Structural properties and hypoglycaemic activity of polysaccharides extracted from the fruits of *Lycium barbarum* L. using various extraction media. *Ind. Crop. Prod.* 188:115725. doi: 10.1016/j.indcrop.2022.115725

Li, G. Q., Chen, P. F., Zhao, Y. T., Zeng, Q., Ou, S. Y., Zhang, Y. H., et al. (2021). Isolation, structural characterization and anti-oxidant activity of a novel polysaccharide from garlic bolt. *Carbohydr. Polym.* 267:118194. doi: 10.1016/j.carbpol.2021.118194

Li, Y. M., Guo, X. X., Zhong, R. F., Ye, C. M., and Chen, J. (2023). Structure characterization and biological activities evaluation of two hetero-polysaccharides from *Lepista nuda*: cell antioxidant, anticancer and immune-modulatory activities. *Int. J. Biol. Macromol.* 244:125204. doi: 10.1016/j.ijbiomac.2023.125204

Li, Q., Li, W. Z., Gao, Q. Y., and Zou, Y. X. (2017). Hypoglycemic effect of Chinese yam (Dioscorea opposita rhizoma) polysaccharide in different structure and molecular weight. *J. Food Sci.* 82, 2487–2494. doi: 10.1111/1750-3841.13919

Li, J., Niu, D. B., Zhang, Y., and Zeng, X. A. (2020). Physicochemical properties, antioxidant and antiproliferative activities of polysaccharides from *Morinda citrifolia* L. (noni) based on different extraction methods. *Int. J. Biol. Macromol.* 150, 114–121. doi: 10.1016/j.ijbiomac.2019.12.157

Liu, J., Willför, S., and Xu, C. L. (2015). A review of bioactive plant polysaccharides: biological activities, functionalization, and biomedical applications. *Bioact. Carbohydr. Diet. Fibre* 5, 31–61. doi: 10.1016/j.bcdf.2014.12.001

Lv, Q. Q. (2020). Structural characterization, selenylation and physiological activities of polysaccharides from wheat bran. [Dissertation/Master's Thesis]. Hefei: Hefei University of Technology.

Lv, Q. Q., Cao, J. J., Liu, R., and Chen, H. Q. (2021). Structural characterization, α-amylase and α-glucosidase inhibitory activities of polysaccharides from wheat bran. *Food Chem.* 341:128218. doi: 10.1016/j.foodchem.2020.128218

Ma, G. X., Yang, W. J., Mariga, A. M., Fang, Y., Ma, N., Pei, F., et al. (2014). Purification, characterization and antitumor activity of polysaccharides from *Pleurotus eryngii* residue. *Carbohydr. Polym.* 114, 297–305. doi: 10.1016/j.carbpol.2014.07.069

Naveen, J., and Baskaran, V. (2018). Antidiabetic plant-derived nutraceuticals: a critical review. *Eur. J. Nutr.* 57, 1275–1299. doi: 10.1007/s00394-017-1552-6

Niu, G. G., You, G., Zhou, X. Y., Fan, H. L., and Liu, X. L. (2023). Physicochemical properties and *in vitro* hypoglycemic activities of hsian-tsao polysaccharide fractions by gradient ethanol precipitation method. *Int. J. Biol. Macromol.* 231:123274. doi: 10.1016/j.ijbiomac.2023.123274

Pan, Y. H., Wang, M. N., Wang, Z. Q., Huang, X. J., Hu, X. B., Wang, Q., et al. (2023). A novel soluble powder containing high *Dendrobium huoshanense* polysaccharide and its *in vitro* hypoglycemic activities evaluation. *Bioact. Carbohydr. Diet. Fibre* 30:100362. doi: 10.1016/j.bcdf.2023.100362

Peng, X. W., Liu, J. J., Tang, N., Deng, J., Liu, C., Kan, H., et al. (2023). Sequential extraction, structural characterization, and antioxidant activity of polysaccharides from *Dendrocalamus brandisii* bamboo shoot shell. *Food Chem. X.* 17:100621. doi: 10.1016/j.fochx.2023.100621

Pi, T. X., Sun, L. S., Li, W., Wang, W., Dong, M. H., Xu, X. X., et al. (2024). Preparation and characterization of kelp polysaccharide and its research on anti-influenza a virus activity. *Int. J. Biol. Macromol.* 280:135506. doi: 10.1016/j.ijbiomac.2024.135506

Qiu, J. J., Xu, X., Guo, J. Y., Wang, Z. Y., Wu, J. J., Ding, H. Q., et al. (2024). Comparison of extraction processes, characterization and intestinal protection activity of *Bletilla striata* polysaccharides. *Int. J. Biol. Macromol.* 263:130267. doi: 10.1016/j.ijbiomac.2024.130267

Seedevi, P., Ramu Ganesan, A., Moovendhan, M., Mohan, K., Sivasankar, P., Loganathan, S., et al. (2020). Anti-diabetic activity of crude polysaccharide and rhamnose-enriched polysaccharide from *G. lithophila* on Streptozotocin (STZ)-induced in Wistar rats. *Sci. Rep.* 10:556. doi: 10.1038/s41598-020-57486-w

Shao, J. R., Li, T., Zeng, S. Y., Dong, J., Chen, X. Y., Zang, C. X., et al. (2023). The structures of two acidic polysaccharides from *Gardenia jasminoides* and their potential immunomodulatory activities. *Int. J. Biol. Macromol.* 248:125895. doi: 10.1016/j.ijbiomac.2023.125895

Shi, X. D., Huang, J. J., Wang, S. Y., Yin, J. Y., and Zhang, F. (2022). Polysaccharides from *Pachyrhizus erosus* roots: extraction optimization and functional properties. *Food Chem.* 382:132413. doi: 10.1016/j.foodchem.2022.132413

Sila, A., Bayar, N., Ghazala, I., Bougatef, A., Ellouz-Ghorbel, R., and Ellouz-Chaabouni, S. (2014). Water-soluble polysaccharides from agro-industrial by-products: functional and biological properties. *Int. J. Biol. Macromol.* 69, 236–243. doi: 10.1016/j.ijbiomac.2014.05.052

Sims, I. M., Carnachan, S. M., Bell, T. J., and Hinkley, S. F. (2018). Methylation analysis of polysaccharides: technical advice. *Carbohydr. Polym.* 188, 1–7. doi: 10.1016/j.carbpol.2017.12.075

Su, T. (2020). Research on design, synthesis andApplication of novel polysaccharide composite materials. [Dissertation/Master's Thesis]. Nanjing: Nanjing University of Science & Technology.

Tai, G. H., Tang, W. J., and Zhuo, Y. F. (1990). Study on water-soluble polysaccharides in ginseng stem-purification and structure determination of SA1. *Songliao J.* 3, 20–23. doi: 10.16862/j.cnki.issn1674-3873.1990.03.007

Tang, Y. Y., He, X. M., Liu, G. M., Zhen, W., Sheng, J. F., Sun, J., et al. (2023). Effects of different extraction methods on the structural, antioxidant and hypoglycemic properties of red pitaya stem polysaccharide. *Food Chem.* 405:134804. doi: 10.1016/j.foodchem.2022.134804

Tang, N. Y., Wang, X. M., Yang, R., Liu, Z. M., Liu, Y. X., Tian, J. J., et al. (2022). Extraction, isolation, structural characterization and prebiotic activity of cell wall polysaccharide from *Kluyveromyces marxianus*. *Carbohydr. Polym.* 289:119457. doi: 10.1016/j.carbpol.2022.119457

Tian, R., Zhang, Y. Z., Cheng, X. B., Xu, B. J., Wu, H. T., Liang, Z. Q., et al. (2023). Structural characterization, and *in vitro* hypoglycemic activity of a polysaccharide from the mushroom *Cantharellus yunnanensis*. *Int. J. Biol. Macromol.* 253:127200. doi: 10.1016/j.ijbiomac.2023.127200

Wang, Z. C. (2021). Study on extraction technology of ginsenosides from stems and leaves of *Panax ginseng* and bioactivity of its polysaccharides and lignocellulose. [Master's Thesis]. Changchun: Jilin Agricultural University.

Wang, J. W., Cheng, X. L., Li, T. D., Song, M. Y., Wang, S. Q., Wen, T. C., et al. (2024). Structural characterization of polysaccharides from *Dictyophora rubrovolvata* mycelium and their immunostimulatory activity in RAW264.7 cells. *Process Biochem.* 139, 22–32. doi: 10.1016/j.procbio.2024.01.024

Wang, J. Y., Wang, X., Xiu, W. Y., Zhou, Z., Yu, S. Y., Yang, M. Y., et al. (2024). The sweet corn cob selenium polysaccharide alleviates type 2 diabetes via modulation of LPS/IκBα/NFκB and the intestinal microbiota. *Food Biosci.* 58:103742. doi: 10.1016/j.fbio.2024.103742

Wang, S. H., Yang, Y. J., Wang, Q., Wu, Z. Q., Liu, X. J., Chen, S. X., et al. (2023). Structural characterization and immunomodulatory activity of a polysaccharide from finger citron extracted by continuous phase-transition extraction. *Int. J. Biol. Macromol.* 240:124491. doi: 10.1016/j.ijbiomac.2023.124491

Wu, J. W., Li, P., Tao, D. B., Zhao, H. T., Sun, R. Y., Ma, F. M., et al. (2018). Effect of solution plasma process with hydrogen peroxide on the degradation and antioxidant activity of polysaccharide from *Auricularia auricula*. *Int. J. Biol. Macromol.* 117, 1299–1304. doi: 10.1016/j.ijbiomac.2018.05.191

Wu, Z. W., Peng, X. R., Liu, X. C., Wen, L., Tao, X. Y., Al-Romaima, A., et al. (2024). The structures of two polysaccharides from *Lepidium meyenii* and their

immunomodulatory effects via activating NF-κB signaling pathway. *Int. J. Biol. Macromol.* 269:131761. doi: 10.1016/j.ijbiomac.2024.131761

Wu, J. Y., Zheng, W. Y., Luo, P., Lin, Z., Li, F. P., Liang, L. L., et al. (2024). Structural characterization of a water-soluble acidic polysaccharide CSP-IV with potential anticoagulant activity from fruit pulp of *Clausena lansium* (Lour.) Skeels Guifei. *Int. J. Biol. Macromol.* 254:128029. doi: 10.1016/j.ijbiomac.2023.128029

Xu, Y. Q., Guo, Y. Y., Gao, Y. K., Niu, X. J., Wang, L. B., Li, X. G., et al. (2018). Seperation, characterization and inhibition on α-glucosidase, α-amylase and glycation of a polysaccharide from blackcurrant fruits. *LWT* 93, 16–23. doi: 10.1016/j.lwt.2018.03.023

Yang, M., Cui, Z. Y., and Wang, B. X. (1991). Study on hypoglycemic effect of ginseng stem and leaf polysaccharide. *Chin. Trad. Patent Med.* 12, 24–25.

Yang, L. Q., Fu, S. S., Zhu, X. N., Zhang, L. M., Yang, Y. R., Yang, X. M., et al. (2010). Hyperbranched acidic polysaccharide from green tea. *Biomacromolecules* 11, 3395–3405. doi: 10.1021/bm100902d

Ye, C. (2007). Preparation and structural analysis of high molecular weight *Schizophyllan*. [Dissertation/Master's Thesis]. Wuhan: Huazhong University of Science and Technology.

Yu, C. X., Ahmadi, S., Shen, S. H., Wu, H. X., Xiao, H., Ding, T., et al. (2022). Structure and fermentation characteristics of five polysaccharides sequentially extracted from sugar beet pulp by different methods. *Food Hydrocolloids.* 126:107462. doi: 10.1016/j.foodhyd.2021.107462

Yuan, G. X., Wang, Y. T., Niu, H. M., Ma, Y., and Song, J. X. (2024). Isolation, purification, and physicochemical characterization of Polygonatum polysaccharide and its protective effect against CCl4-induced liver injury via Nrf2 and NF-κB signaling pathways. *Int. J. Biol. Macromol.* 261:129863. doi: 10.1016/j.ijbiomac.2024.129863

Zhang, X. H., Hu, Z. Y., Duan, Y. Q., Jiang, Y. X., Xu, W. W., Yang, P. C., et al. (2024). Extraction, characterization, and neuroprotective effects of polysaccharides the stems of *Panax ginseng* CA Meyer by three different solvents (water, acid, alkali). *Ind. Crop. Prod.* 222:119512. doi: 10.1016/j.indcrop.2024.119512

Zhang, L., Kong, H. C., Li, Z. F., Ban, X. F., Gu, Z. B., Hong, Y., et al. (2023). Physicochemical characterizations, α-amylase inhibitory activities and inhibitory mechanisms of five bacterial exopolysaccharides. *Int. J. Biol. Macromol.* 249:126047. doi: 10.1016/j.ijbiomac.2023.126047

Zhang, J., Wang, S. Z., Yang, M. R., Ding, J. M., Huang, Y. Z., Zhu, Y. D., et al. (2024). Antiviral activity of a polysaccharide from Sargassum fusiforme against respiratory syncytial virus. *Int. J. Biol. Macromol.* 279:135267. doi: 10.1016/j.ijbiomac.2024.135267

Zhang, F., Xu, Y. Q., Bu, X. Y., Wang, Z. T., Qi, S. L., Li, D. L., et al. (2023). A novel procedure for simultaneous extraction of polysaccharides and polyphenols from *Schisandra Chinensis*: modeling, characterization and biological properties. *Ind. Crop. Prod.* 193:116208. doi: 10.1016/j.indcrop.2022.116208

Zhang, Y., Yang, B. J., Sun, W., Sun, X., Zhao, J., and Li, Q. H. (2024). Structural characterization of squash polysaccharide and its effect on STZ-induced diabetes mellitus model in MIN6 cells. *Int. J. Biol. Macromol.* 270:132226. doi: 10.1016/j.ijbiomac.2024.132226

Zhao, M. M., Bai, J. W., Bu, X. Y., Yin, Y. T., Wang, L. B., Yang, Y., et al. (2021). Characterization of selenized polysaccharides from *Ribes nigrum L.* and its inhibitory effects on α-amylase and α-glucosidase. *Carbohydr. Polym.* 259:117729. doi: 10.1016/j.carbpol.2021.117729

Zhao, X. X., Wang, J. H., Ye, S. H., Liu, Y., and Zhang, L. L. (2009). Effect of ginseng stem and leaf polysaccharide on immune function in mice. *China Brewing* 3, 56–58. doi: 10.3969/j.issn.0254-5071.2009.03.017

Zhao, J. L., Zhang, M. P., and Zhou, H. L. (2019). Microwave-assisted extraction, purification, partial characterization, and bioactivity of polysaccharides from *Panax ginseng*. *Molecules* 24:1605. doi: 10.3390/molecules24081605

Zhou, W., Han, L. J., Raza, S. H. A., Yue, Q. M., Sun, S. N., Zhao, Y. X., et al. (2023). Polysaccharides in *Berberis dasystachya* improve intestinal flora depending on the molecular weight and ameliorate type 2 diabetes in rats. *J. Funct. Foods* 100:105381. doi: 10.1016/j.jff.2022.105381

Zou, M. Y., Hu, X. B., Wang, Y. J., Wang, J. H., Tang, F. Y., and Liu, Y. (2022). Structural characterization and anti-inflammatory activity of a pectin polysaccharide HBHP-3 from *Houttuynia cordata*. *Int. J. Biol. Macromol.* 210, 161–171. doi: 10.1016/j.ijbiomac.2022.05.016